Polymer Journal, Vol. 39, No. 12, pp. 1253–1273 (2007)

SPECIAL ISSUES -PROGRESS IN STRUCTURE ANALYSES OF POLYMERIC MATERIALS BY SYNCHROTRON RADIATION AND NEUTRON BEAM-

Structural Refinement and Extraction of Hydrogen Atomic Positions in Polyoxymethylene Crystal Based on the First Successful Measurements of 2-Dimensional High-Energy Synchrotron X-ray Diffraction and Wide-Angle Neutron Diffraction Patterns of Hydrogenated and Deuterated Species

Kohji TASHIRO,[1,†] Makoto HANESAKA,[1] Takashi OHHARA,[2] Tomoji OZEKI,[3] Toshiaki KITANO,[4] Takashi NISHU,[4] Kazuo KURIHARA,[2] Taro TAMADA,[2] Ryota KUROKI,[2] Satoru FUJIWARA,[2] Ichiro TANAKA,[5] and Nobuo NIIMURA[5]

[1]*Department of Future Industry-oriented Basic Science and Materials, Graduate School of Engineering, Toyota Technological Institute, Tempaku, Nagoya 468-8511, Japan*
[2]*Research Unit for Quantum Beam Science Initiative, Japan Atomic Energy Agency, Tokai-mura, Naka-gun 319-1195, Japan*
[3]*Department of Chemistry and Materials Science, Graduate School of Science and Engineering, Tokyo Institute of Technology, Meguro, Tokyo 152-8551, Japan*
[4]*Department of Applied Chemistry, Graduate School of Engineering, Nagoya University, Chikusa, Nagoya 464-8603, Japan*
[5]*Graduate School of Science and Engineering Institute of Applied Beam, Ibaraki University, Mito 310-8512, Japan*

(Received June 15, 2007; Accepted August 3, 2007; Published October 10, 2007)

ABSTRACT: 2-Dimensional X-ray and neutron diffraction patterns have been successfully measured for deuterated and hydrogenated polyoxymethylene (POM) samples obtained by γ-ray induced solid-state polymerization reaction. More than 700 reflections were collected from the X-ray diffraction data at $-150\,^{\circ}C$ by utilizing a high-energy synchrotron X-ray beam at SPring-8, Japan, from which the crystal structure of POM has been refined thoroughly including the extraction of hydrogen atomic positions as clearly seen in the difference Fourier synthesis map. As the first trial the nonuniform (9/5) helical model was analyzed with the reliability factor (R factor) 6.9%. The structural analysis was made also using the X-ray reflections of about 400 observed at room temperature (R 8.8%), and the thermal parameters of constituent atoms were compared between the low and high temperatures to discuss the librational thermal motion of the chains. The 2-dimensional neutron diffraction data, collected for the deuterated and hydrogenated POM samples using an imaging plate system specifically built-up for neutron scattering experiment, have allowed us to pick up the D and H atomic positions clearly in the Fourier synthesis maps. Another possible model, (29/16) helix, which was proposed by several researchers, has been also investigated on the basis of the X-ray diffraction data at $-150\,^{\circ}C$. The direct method succeeded in extracting this (29/16) model straightforwardly. The R factor was 8.6%, essentially the same as that of (9/5) helical model. This means that the comparison of the diffraction intensity between the data collected from the full-rotation X-ray diffraction pattern and the intensity calculated for both the (9/5) and (29/16) models cannot be used for the unique determination of the superiority of the model, (9/5) or (29/16) helix. However, we have found the existence of 001 and 002 reflections which give the longer repeating period 55.7 Å. Besides there observed a series of meridional *00l* reflections forbidden for (9/5) helical model. These additional evidences support the nonuniform (29/16) helical model as the most plausible chain conformation of POM crystal.
[doi:10.1295/polymj.PJ2007076]

KEY WORDS Polyoxymethylene / Synchrotron X-ray Diffraction / Wide-angle Neutron Diffraction / Deuterated Species / Structure Analysis / Fourier Synthesis / Hydrogen Atoms /

Quantitative evaluation of ultimate physical properties of crystalline polymers is essentially important as a guiding principle for the development of polymer materials with more excellent properties than before. Typical examples can be seen in the development of ultra-drawn polymer materials with extremely high Young's modulus along the draw axis. The evaluation of the ultimate elastic constants, in particular, the crystallite modulus or a Young's modulus of a crystal lattice along the chain axis was made both experimentally and theoretically.[1,2] As for the experimental evaluation of the mechanical properties is referred to the literature.[1,2] In the theoretical evaluation we start the calculation using the information on the atomic coor-

[†]To whom correspondence should be addressed (Tel: +81-52-809-1790, Fax: +81-52-809-1793, E-mail: ktashiro@toyota-ti.ac.jp).

dinates in crystal lattice and the interatomic interactions. The atomic positions adopted in the theoretical calculation should be as accurate as possible. Unfortunately, however, the crystal structure information of partially crystalline polymer materials, which is generally obtained by the X-ray structure analysis, is relatively low in its reliability compared with the cases of low-molecular-weight compounds. In the latter case we prepare a single crystal of sub-millimeter size, which gives several thousands of sharp X-ray reflections, giving an accurate crystal structure after a rapid analysis using a convenient software. In contrast, the polymer samples give usually only several tens of reflections at most. These reflections are broad and diffuse, making it difficult to perform the quantitative and exact evaluation of integrated intensities of the observed reflections. As a result, it is very hard to build up a starting model necessary for the structural determination. Additionally, the total number of the observed X-ray reflections is too small to perform the refinement of the thus obtained initial structure model. A measure of structural accuracy is expressed using a reliability factor or R factor, which is defined as a measure of agreement between the observed and calculated reflection intensities. The structure of low-molecular-weight compound is analyzed in general with R factor lower than *ca.* 5%, whereas the R factor is in a range of 10–20% for crystalline polymer materials, indicating a lower accuracy in the analyzed structure.

In addition, the accurate structural analysis of low-molecular-weight compounds can give us an information of hydrogen atomic positions, which is very important for the theoretical evaluation of anisotropy in three-dimensional elastic constants of the crystal lattice, for example, because the hydrogen atoms are mostly located at the outermost positions of molecules and the nonbonded H$\cdots$H interactions govern the mechanical properties of crystal. Unfortunately the determination of hydrogen atomic position is quite difficult even for the low-molecular-weight compounds because the X-ray scattering power of hydrogen atom is much lower than those of carbon, oxygen and so on. Of course it had been practically impossible for a long time to determine the hydrogen atomic positions for the crystalline polymer materials in general.

How to increase the Reliability of Crystal Structure of Polymer

In order to increase the reliability of structure information of polymer crystals, the various kinds of method had been developed so far, which were reviewed in the literature.[3] In such trials the present authors also have made an effort for this purpose. One of the most important keys to improve the structure analysis is to increase the total number of observed reflections. We introduced an imaging plate for the quantitative collection of 2-dimensional X-ray diffraction patterns of the oriented polymer samples.[4,5] One of the most useful features of the imaging plate detector is in its wide dynamic range of photon counting.[6,7] That is to say, the reflection signal can be estimated in a linear scale in a wide range of 1 to 10^6 photons. Besides the integration of the broad and diffuse reflections can be made relatively easily since the collected diffraction pattern is saved as digitized data treatable by a computer. As reported already, we developed a software for this purpose. At the same time we used an X-ray beam of shorter wavelength as positively as possible; Mo-Kα line (0.71073 Å) instead of Cu-Kα line (1.54178 Å). As a result the total number of observed reflections was increased almost twice. Recently we have used a high energy synchrotron radiation as an incident X-ray beam of much shorter wavelength, 0.3282 Å. This allowed us to collect several to ten times larger number of observed reflections. The usefulness of this technique will be illustrated concretely in the present paper.

Another important point for increasing the reflection number is to measure the X-ray diffraction data at lower temperature. The thermal motion of atoms is ceased at low temperature, allowing us to collect more number of sharper reflections over a wider region of diffraction angle. In this way a combination of strong X-ray beam of shorter wavelength with a highly sensitive 2-dimensional imaging plate detector for the diffraction measurement at low temperature is one of the most useful methods to collect the larger number of sharper reflections in a wider scattering angle region. For the quantitative analysis of the thus collected reflection data, we developed a software, in which the overlapped reflections can be separated effectively, and the integrated intensity of individual reflection can be estimated accurately.[4,5] Using these reflection data, for the first time, we can succeed to obtain the initial model on the basis of a so-called direct method as reported for the several kinds of polymer crystals.[4,5] In some cases we could extract even the hydrogen atomic positions successfully.

To Extract Hydrogen Atoms

In this way the collection of larger number of reflections is decisively useful for the derivation of accurate structural models. But, even in the case of low-molecular-weight compounds, the determination of hydrogen atomic positions is still difficult. As a positive action for this purpose, a utilization of deuterated sample species in the neutron diffraction measurement is very useful.[8] But, the above-mentioned various situations in the diffraction experiments of

polymers are seen in the neutron experiment also. It is desirable to use the 2-dimensional highly-sensitive digital detector for the collection of broad neutron diffraction data of deuterated polymer samples. Recently Niimura *et al.* developed a new wide-angle neutron diffraction system, where a highly-sensitive imaging plate was used for the collection of 2-dimensional diffraction data for the quantitative analysis.[9,10] In the previous paper we reported the first success to extract the exact hydrogen atomic positions for orthorhombic polyethylene crystal on the basis of wide-angle neutron diffraction data collected using this system for the uniaxially-orineted deuterated sample.[11] Because of the limitation in choosing the neutron beam of shorter wavelength (1.51 Å in our case) and the relatively weaker beam intensity compared with the X-ray beam, the total number of reflections observable using this system is much lower than that obtained by the X-ray method. Therefore an accurate structure analysis using only the neutron diffraction data is still difficult for the polymer samples. Rather it may be general to combine the X-ray and neutron diffraction data collected for the deuterated samples for getting the most reliable structure information including the hydrogen atom positions. That is, the structure analysis is made at first using an X-ray diffraction data as mentioned above, and then the hydrogen atomic positions are determined on the basis of neutron diffraction data with the heavier atoms fixed at the X-ray analyzed positions.[11] For many polymers, however, it is difficult experimentally (and financially) to synthesize the deuterated polymer species in a large scale. In the neutron experiment, we have to prepare the uniaxially-oriented deuterated samples with diameter of several millimeter to increase the signal-to-noise ratio of the diffraction data. Sometimes a utilization of normal hydrogenated polymer samples might be useful also for the extraction of hydrogen atomic positions.[11] In this case the hydrogen atom peak can be found out as a peak of negative height because the light hydrogen atom possesses a negative scattering cross section different from the positive cross section of heavy hydrogen atom or deuterium. But this method is sometimes disturbed by the larger contribution of incoherent neutron scattering from light hydrogen atom, which is overwhelmingly strong compared with the corresponding coherent scattering intensity.

Purpose of the Present Paper

In order to demonstrate the usefulness of the various techniques mentioned above in the structure analysis of polymer crystals, we will report here the case study of polyoxymethylene (POM), in which the fully crystalline and perfectly oriented samples, obtained by γ-ray induced solid-state polymerization reaction of trioxane (TOX) and tetraoxane (TOM) single crystals, were used.[12,13] For the X-ray diffraction measurement we have performed the experiment for the hydrogenated POM sample at $-150\,^{\circ}$C as well as at room temperature using a combination of high-energy synchrotron-sourced X-ray beam of short wavelength and the 2-dimensional imaging plate detector. The total number of the thus-collected X-ray reflections exceeded 700, far beyond the number of reflections reported so far, making it possible to refine the crystal structure of POM at high accuracy. For the wide-angle neutron diffraction measurement, deuterated POM samples obtained from the γ-ray solid-state polymerization reaction of deuterated TOX single crystals were used in addition to the normal hydrogenated samples. The diffraction data were collected at room temperature using a neutron imaging plate system. As a result we have succeeded to clarify the accurate positions of hydrogen (and deuterium) atoms.

It may be important to mention here the not-yet-solved problems in crystal structure analysis of POM, although many papers had been reported so far. Tadokoro and his coworkers analyzed the POM crystal structure using a γ-ray polymerized sample and proposed a trigonal structure of (9/5) uniform helix.[14–16] Carazzolo pointed out the uneven interlayer spacings in the X-ray fiber diagram of uniaxially-oriented POM sample, and they estimated the accurate fiber period, from which they proposed a uniform helical model of longer period, (29/16) helix with the fiber period of 56 Å.[17] By detecting some meridional *00l* reflections forbidden for the uniform (9/5) helical model, Saruyama *et al.* introduced a disorder into a uniform model: about 18 segments form a uniform helical segment and these segments are unwinded at the boundary between the adjacent regular helical segments by about 20°.[18,19] This model can be approximated as a uniform (324/179) helical model, which is essentially equivalent to the (29/16) helical model proposed by Carazzolo.[17] These three kinds of model assumed a uniformity of helical segment in a longer or shorter range along the chain axis. But, why do we need to assume the uniform helical symmetry in the crystal lattice? Strictly speaking, the unit cell of POM has only a 3_1 (3_2) screw axis along the chain axis when we assume the space group $P3_2$.[4] That is to say, the 3 successive monomeric units should be included as one crystallographically asymmetric unit, and so the geometry of these 3 monomeric units is not necessarily equal to each other. The situation is more serious for (29/16) helical model, which may be packed in the crystal lattice with the lowest space-group symmetry or $P1$. In the present paper we will discuss these points also on the basis of X-ray diffraction data in addition to the description about the

refined structure analysis of POM crystal based on the (9/5) helical model as the initial motivation of the discussion. This is because these various kinds of models are very difficult to distinguish from each other by means of the comparison of the observed and calculated intensities based on the X-ray (and neutron) fiber diagrams only. In the last section we will discuss the superiority of (29/16) helical model on the basis of the newly-measured X-ray diffraction data.

Anyway, as seen later, the present research is the first success to describe the detailed structure of POM crystal including the hydrogen atomic positions on the basis of the thoroughly-performed analysis of the synchrotron-sourced X-ray diffraction data and the neutron diffraction data collected for both the deuterated and hydrogenated sample species obtained by γ-ray-induced solid-state polymerization reactions of monomer single crystals.

EXPERIMENTAL SECTION

Samples

Hydrogenated POM (POM-h_2) and deuterated POM (POM-d_2) samples were obtained by the solid-state polymerization reactions of hydrogenated and deuterated trioxane (TOX) single crystals under the γ-ray irradiation (^{60}Co, 6kGy at 60 °C).[12,13] The thus-obtained POM samples contained some portions of twin structures.[13,20,21] These twin structures could be erased almost perfectly by heating the original sample at 170 °C for 5 h. In case of POM-h_2, the sample was relatively easily thermally decomposed and it became thinner after a long heat treatment. In contrast, the POM-d_2 was found to keep the original size relatively stably even when heated up to high temperature. The thus prepared POM-h_2 and POM-d_2 samples without any twin structures were transferred to the neutron diffraction measurements. For the X-ray diffraction measurements the POM-h_2 samples produced from the tetraoxane (TOM) single crystal were used, which were polymerized under almost the same condition as that of TOX and contained no twin structure.[13,21]

Measurements

Wide-angle X-ray diffraction (WAXD) measurement was performed at a beam line BL04B2 of SPring-8, Hyogo, Japan. A high-energy X-ray source of 0.3282 Å wavelength was utilized, very short compared with the conventional X-ray beam used in the laboratory (0.71073 Å for Mo-Kα and 1.5418 Å for Cu-Kα). The full-rotation diffraction patterns were collected at −150 °C and room temperature using an imaging plate detector set in a Weissenberg camera of 12 cm radius (MAC Science, Japan). The full-rotation method, in which the POM sample was rotated 360° around the chain axis during the exposure to X-ray beam, was utilized here because the POM sample was not a single crystal but a polycrystal of 100% crystallinity and perfect *c*-axial orientation. The sample used there was POM-h_2 obtained from the polymerization of TOM single crystal.

2-Dimensional wide-angle neutron diffraction (WAND) measurement was performed at room temperature using a BIX-3 system (high resolution neutron diffractometer dedicated to biological macromolecules) built up in the JRR-3 reactor hall of Japan Atomic Energy Agency. The details of the system were already described in the previous paper.[11] The sample was set vertically on a goniometer head on the top of the cylindrical camera of 40 cm diameter. An imaging plate was initially positioned around the sample. The monochromatized neutron beam with a wavelength 1.51 Å was incident on the sample through a slit of 3 mm diameter. After 6–24 h exposure, the imaging plate was moved continuously to the lower part of the camera, during which the reflection data were read out by irradiating a He-Ne laser beam.

Data Analysis

The thus collected 2-D diffraction patterns were analyzed using a home-made software.[4,5] The position and integrated intensity of a reflection were evaluated after separating an overlap of neighboring reflections. The integrated intensity was corrected for the Lorentz and polarization factors for X-ray diffraction data and for the Lorentz factor for neutron data. No correction was made for the absorption effect for both the cases. The structure factors were evaluated by taking the multiplicity into account.

Structure Analysis

Determination of unit cell parameters and the indexing of the observed reflections were made using the above-mentioned software.[4,5] The thus-collected sets of (h, k, l) and structure factor $F(hkl)$ were transferred to a software of crystal structure analysis, WinGX (version 1.70.01).[22] The direct method was applied to find out the initial model by using a SHLEX-97 (SHELXS).[23] Least squares refinement was made on the basis of the full matrix method using a software SHELXL of SHELX-97. The reflections satisfying the cut-off condition of $|F_o| > 4\sigma(|F_o|)$ were used in the least squares refinement. Here $|F_o|$ and $\sigma(|F_o|)$ are an absolute value of the observed structure factor and the corresponding standard error, respectively. The reliability of the structure analysis was evaluated by the reliability factors defined by the following equation: $R = \Sigma||F_o|^2 - |F_c|^2|/\Sigma|F_o|^2$, where $|F_c|$ is the calculated structure factor.

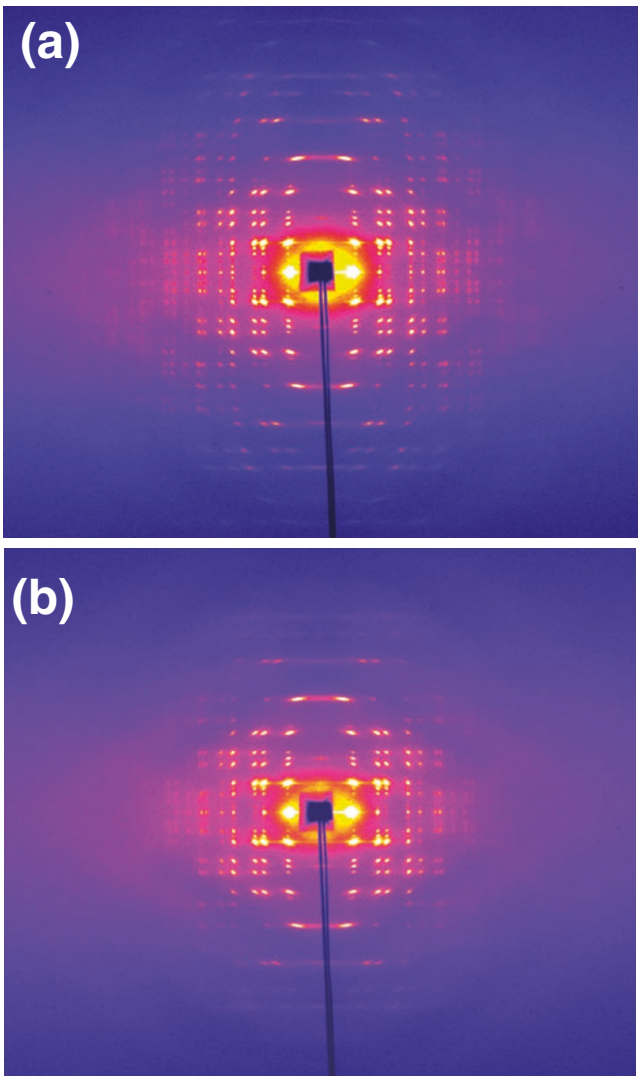

Figure 1. Full-rotation X-ray diffraction diagrams of solid-state-polymerized polyoxymethylene (POM-h_2) measured with the synchrotron X-ray beam of 0.3282 Å wavelength at (a) −150 °C and (b) room temperature. The vertical direction is parallel to the *c* axis.

RESULTS AND DISCUSSION

Figure 1 shows the full-rotation X-ray diffraction diagrams taken for POM samples where the vertical axis is parallel to the chain axis. When Cu-Kα and Mo-Kα beams were used as incident X-ray sources, the total number of observed reflections was only 70 and 270 at most in the first quadrant, respectively.[4] The synchrotron-sourced X-ray beam of 0.3282 Å wavelength gave the reflections covering the equatorial line to the 33rd layer line or the 774 reflections at −150 °C and 428 reflections at room temperature (0–28th lines). These reflections were analyzed using the homemade software,[4,5] and the positions and integrated intensities were evaluated as accurately as possible. The number of unique reflections was 202 at −150 °C and 107 at room temperature.

As pointed out in the introductory session, there had been proposed several models for POM chain conformation, regular 9/5 helix,[14–16] regular 29/16 helix,[17] 38/21 helix,[24] and a helix with defects at constant intervals which is approximated to be a uniform 324/179 helix.[18,19] The latter three models, under the assumption of uniform helix, are essentially the same: the number of monomeric units per one turn is about 1.81, which is different by only 0.01 from the regular 9/5 helical conformation model. In the first several sections we will analyze the crystal structure of POM based on the (9/5) helical model as mentioned in the introductory section. When the space group $P3_2$ is assumed, the 3 monomeric units are included as a crystallographically asymmetric unit and the uniformity of (9/5) helix is now lost and the molecular chain possesses only 3_1 (3_2) symmetry axis. The total number of structure parameters to be determined is 109 at maximum: the (x, y, z) coordinates and anisotropic thermal parameters (U_{ij}, i and $j = 1$–3) for each atom and the scale factor (9 parameters × 12 atoms + scale factor = 109 parameters). If the isotropic thermal parameters are assumed, the total number of parameters is 49 ($4 \times 12 + 1$). About 200 unique reflections, which were picked up from the 700 reflections observed, were used for these analyses. If we try to analyze the nonuniform (29/16) helical model, the adjustable parameters are tremendously large. The discussion about the (29/16) helical model will be given in a later section.

Structure Analysis Using WAXD Data

The unit cell parameters determined are $a = b = 4.464(4)$ Å, c (fiber axis) = 17.389(2) Å and $\gamma = 120°$ at room temperature, and $a = b = 4.373(4)$ Å, c (fiber axis) = 17.274(2) Å and $\gamma = 120°$ at −150 °C. The initial models were obtained successfully by the direct method, which were transferred to the structure refinement using 184 reflections for the −150 °C data and 106 reflections for the room temperature data under the condition of sigma cut-off 4 ($|F_o| > 4\sigma(|F_o|)$). The refinement was performed at first for the atomic coordinates of C and O atoms with the anisotropic thermal parameters U_{ij}. The so-called differential Fourier synthesis (*Fo–Fc*) was carried out to extract the hydrogen atomic positions, where *Fc* is the structure factor calculated for the C and O atoms. The refinement was made again for all the coordinates of C, O and H atoms and the anisotropic (for C and O atoms) and isotropic thermal parameters (for H atoms). The final reliability factor was 6.9% for the data at −150 °C and 8.8% for the data at room temperature. The thus-determined atomic coordinates and thermal parameters are given in Table I(a) and I(b) for the data at −150 °C and room temperature, respec-

Table I. Fractional Coordinates and Thermal Parameters of POM Crystal (POM-h_2) at (a) −150 °C and (b) Room Temperature on the basis of (9/5) Helical Model

(a) −150 °C

Atom	x/a	y/b	z/c	$U_{(eqv)}$/Å$^{2a)}$
C(1)[b)]	−0.0184(3)	0.1468(2)	0.06536(8)	0.0229(2)
O(2)	−0.1656(2)	−0.1249(3)	0.11929(6)	0.0284(2)
C(3)	0.0823(3)	−0.0977(3)	0.17663(9)	0.0276(2)
O(4)	0.1356(3)	0.1599(3)	0.23268(6)	0.0288(2)
C(5)	−0.1388(3)	0.0318(3)	0.28741(8)	0.0237(2)
O(6)	−0.0936(3)	−0.1746(2)	0.34292(5)	0.0275(2)
H(1)	−0.193(7)	0.182(7)	0.040(2)	0.064(8)
H(2)	0.110(8)	0.363(7)	0.090(2)	0.066(9)
H(3)	0.271(10)	−0.094(8)	0.150(4)	0.126(11)
H(4)	−0.070(9)	−0.338(9)	0.209(3)	0.102(10)
H(5)	−0.370(7)	−0.103(8)	0.263(2)	0.071(9)
H(6)	−0.162(7)	0.206(7)	0.310(2)	0.053(8)

Atom	U_{11}	U_{22}	U_{33}	U_{23}	U_{13}	U_{12}/Å^2
C(1)	0.0268(4)	0.0208(3)	0.0189(3)	0.0057(3)	0.0006(3)	0.0101(3)
O(2)	0.0248(3)	0.0394(4)	0.0189(3)	−0.0060(3)	−0.0033(3)	0.0145(3)
C(3)	0.0426(4)	0.0352(4)	0.0193(3)	−0.0018(3)	0.0048(3)	0.0302(3)
O(4)	0.0281(3)	0.0329(4)	0.0206(3)	0.0090(3)	0.0036(3)	0.0117(3)
C(5)	0.0300(3)	0.0281(4)	0.0184(3)	0.0033(3)	−0.0032(3)	0.0186(3)
O(6)	0.0330(3)	0.0266(4)	0.0152(3)	−0.0060(3)	−0.0065(3)	0.0091(3)

(b) Room Temperature

Atom	x/a	y/b	z/c	$U_{(eqv)}$/Å^2
C(1)	1.0936(18)	0.1792(14)	−0.1891(5)	0.0407(18)
O(2)	0.8433(14)	−0.0435(15)	−0.1330(4)	0.0531(17)
C(3)	0.966(2)	−0.1657(18)	−0.0783(5)	0.0450(19)
O(4)	1.1658(14)	0.0917(14)	−0.0219(3)	0.0534(19)
C(5)	0.9857(19)	0.1447(17)	0.0339(5)	0.0438(16)
O(6)	0.8545(17)	−0.1315(18)	0.0879(4)	0.0564(18)
H(1)	1.012(12)	0.355(16)	−0.205(5)	0.026(18)
H(2)	1.321(12)	0.319(14)	−0.161(7)	0.024(17)
H(3)	1.15(2)	−0.24(2)	−0.096(7)	0.08(3)
H(4)	0.813(17)	−0.342(15)	−0.056(6)	0.030(18)
H(5)	1.155(18)	0.347(19)	0.060(7)	0.05(2)
H(6)	0.750(17)	0.15(2)	0.011(8)	0.06(2)

Atom	U_{11}	U_{22}	U_{33}	U_{23}	U_{13}	U_{12}/Å^2
C(1)	0.060(4)	0.017(2)	0.035(3)	0.005(3)	0.006(3)	0.011(2)
O(2)	0.052(3)	0.067(3)	0.031(2)	−0.011(3)	−0.015(3)	0.023(2)
C(3)	0.057(3)	0.044(3)	0.023(2)	−0.003(3)	0.007(3)	0.017(3)
O(4)	0.050(3)	0.055(3)	0.035(3)	0.004(3)	0.011(3)	0.011(2)
C(5)	0.076(3)	0.044(2)	0.032(3)	0.007(3)	−0.001(3)	0.046(2)
O(6)	0.074(3)	0.069(3)	0.026(3)	−0.010(3)	−0.003(3)	0.035(3)

a) $U_{(eqv)} = 1/3\Sigma\Sigma[U_{ij}a_i^*a_j^*a_ia_j\cos(\tau_{ij})$, where U_{ij} is the component of an isotropic thermal parameter tensor. a^* and a are respectively the unit cell vectors of the reciprocal lattice and the real lattice. b) The numbering of atoms is shown below.

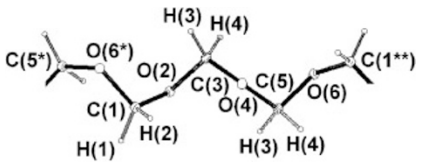

tively. Table II shows the comparison in structure factor between the observed and calculated values. Figure 2 shows the crystal structure determined at −150 °C. Figure 3(a) shows the Fourier map obtained for a single chain by using the *Fo* data, and Figure 3(b) gives the Fourier map derived from the

Table II. Comparison of Structure Factor between Observed and Calculated Values for the Structure of POM Crystal (POM-h_2) at (a) −150 °C and (b) Room Temperature

(a) −150 °C

h	*k*	*l*	|*Fo*|	|*Fc*|	*Phase*/°
0	1	0	73.97	72.30	0.1
−1	2	0	15.23	15.02	359.1
0	2	0	3.72	2.92	358.7
−1	3	0	9.18	10.28	180.1
0	3	0	11.19	11.82	182.2
−2	4	0	9.10	10.40	178.8
−1	4	0	8.76	9.40	181.7
0	4	0	6.29	5.96	185.6
−2	5	0	4.18	3.76	180.9
−1	5	0	1.74	1.58	193.1
0	5	0	1.38	1.22	343.8
−3	6	0	1.15	0.75	5.0
−2	6	0	1.33	1.38	354.1
−1	6	0	2.32	2.49	356.8
0	6	0	4.03	2.76	1.2
−3	7	0	2.29	1.78	358.8
−2	7	0	1.18	1.95	358.5
1	1	1	4.05	3.28	242.0
−3	2	1	4.35	4.3	110.2
−2	2	1	4.92	3.69	71.5
2	2	1	2.52	2.54	246.1
−4	3	1	1.82	2.18	118.0
−3	3	1	2.91	2.68	82.0
−3	2	2	3.34	3.80	205.4
2	2	2	4.43	5.37	136.4
−5	3	2	5.59	5.3	231.4
−4	3	2	5.31	5.71	190.0
−3	3	2	4.28	4.83	136.2
3	3	2	2.87	3.50	142.9
−6	4	2	2.88	3.27	219.4
−5	4	2	5.19	4.96	181.8
−4	4	2	5.88	5.73	136.6
−6	5	2	2.38	2.51	179.8
−5	5	2	4.68	4.06	138.4
−1	1	3	3.28	2.69	282.8
1	1	3	8.42	7.71	187.0
−3	2	3	10.90	10.79	217.3
−2	2	3	9.23	8.60	274.6
2	2	3	8.42	9.78	183.2
−5	3	3	5.69	5.78	196.3
−4	3	3	7.87	9.11	228.8
−3	3	3	10.35	10.1	272.7
−5	4	3	4.63	4.48	228.3
−4	4	3	6.97	7.17	268.5
−5	5	3	2.80	2.40	254.4
−1	1	4	2.80	2.55	343.6
1	1	4	8.82	7.44	65.7
−3	2	4	3.72	4.07	313.7
−2	2	4	7.63	7.08	341.5
−3	3	4	2.16	2.41	341.1
−1	1	5	40.49	38.93	230.8
1	1	5	34.43	32.62	141.6
−3	2	5	12.93	11.79	248.3
−2	2	5	27.06	26.93	229.8
−5	3	5	3.67	5.20	72.3
−3	3	5	5.85	5.35	223.5
3	3	5	2.81	3.42	320.2
−6	4	5	3.00	3.02	59.5
−5	4	5	4.88	5.10	56.4
−4	4	5	4.39	4.67	53.0
−6	5	5	1.88	1.91	38.0
−5	5	5	3.93	3.99	45.2
−1	1	6	1.42	0.95	233.9
1	1	6	1.03	0.45	53.2
−3	2	6	1.27	1.22	320.1
−2	2	6	3.23	2.47	292.3
−3	3	6	2.74	2.31	286.5
−5	3	7	3.32	3.16	126.9
−4	3	7	2.15	2.07	86.4
3	3	7	1.79	3.00	277.4
−7	4	7	1.84	2.04	140.5
−6	4	7	2.60	2.80	108.2
−5	4	7	3.26	2.81	66.7
−4	4	7	2.31	2.21	4.3
−6	5	7	2.16	2.38	54.4
−5	5	7	2.52	2.73	9.0
−6	6	7	3.20	2.06	6.9
−1	1	8	10.96	9.19	324
1	1	8	17.15	15.78	144.1
−3	2	8	14.11	13.82	284.6
−2	2	8	16.24	16.12	324.6
2	2	8	6.73	7.38	134.7
−5	3	8	1.55	1.13	217.2
−4	3	8	6.23	6.60	289.4
−3	3	8	11.52	12.07	320.6
−7	4	8	2.02	2.21	90.6
−6	4	8	2.23	2.47	113.4
−5	4	8	1.60	0.79	203.9
−4	4	8	4.41	4.10	305.3
−6	5	8	2.36	2.28	128.6
−6	6	8	2.85	1.97	138.4
−1	1	9	9.93	9.29	27.2
1	1	9	3.52	4.20	24.3
−2	2	9	1.30	2.01	22.4
−1	1	10	5.05	6.44	106.0
1	1	10	11.8	12.66	281.2
−3	2	10	13.58	13.03	139.2
−2	2	10	13.39	13.69	103.7
2	2	10	8.88	7.29	278.9
−4	3	10	5.74	6.25	124.9
−3	3	10	11.46	11.06	100.9
−7	4	10	2.04	1.99	325.7
−6	4	10	2.39	2.35	317.8
−4	4	10	3.68	3.42	91.4
−6	5	10	1.96	2.46	297.8
−6	6	10	2.98	1.95	282.0
−5	3	11	2.35	2.35	135.5
−4	3	11	1.72	1.85	198.4
−7	4	11	1.79	1.54	101.3
−6	4	11	2.30	2.41	146.1

Continued on the next page.

Continued.

h	*k*	*l*	|*Fo*|	|*Fc*|	*Phase*/°
−5	4	11	2.92	2.68	194.3
−4	4	11	2.86	2.31	252.4
−6	5	11	2.33	2.42	193.5
−5	5	11	1.96	2.79	239.0
−6	6	11	2.69	2.16	225.1
−1	1	13	18.06	16.76	13.9
1	1	13	17.96	16.95	101.1
−3	2	13	7.84	7.90	341.5
−2	2	13	15.51	14.91	9.5
−5	3	13	3.51	3.69	180.5
−4	3	13	1.69	2.35	228.6
−3	3	13	3.79	3.92	344.9
−6	4	13	2.16	2.22	169.1
−5	4	13	4.07	3.99	190.5
−4	4	13	3.71	3.84	208.6
−6	5	13	1.80	1.64	169.7
−5	5	13	3.20	3.41	186.6
−1	1	14	3.60	3.17	258.1
1	1	14	2.55	2.81	167.4
−2	2	14	2.29	2.61	253.9
1	1	15	2.45	2.50	66.4
−3	2	15	5.52	5.54	30.0
−2	2	15	3.67	3.67	335.2
2	2	15	5.22	5.80	62.0
−5	3	15	4.06	3.67	35.9
−4	3	15	5.96	5.96	12.0
−3	3	15	6.48	6.23	335.5
−5	4	15	3.46	3.32	357.0
−4	4	15	5.52	5.14	332.6
−1	1	16	1.27	1.19	12.2
−3	2	16	2.22	1.75	252.2
2	2	16	2.39	3.01	299.2
−5	3	16	3.59	3.53	195.0
−4	3	16	3.31	3.48	243.5
−3	3	16	2.97	3.14	302.2
−6	4	16	2.05	2.34	195.3
−5	4	16	3.77	3.37	240.5
−4	4	16	3.77	3.77	289.1
−6	5	16	1.99	1.88	226.4
−5	5	16	2.96	2.80	275.9
−1	1	18	16.65	15.68	59.2
1	1	18	5.40	5.14	45.9
−3	2	18	4.32	4.44	256.4
−2	2	18	2.02	2.17	16.2
2	2	18	5.42	5.54	241.5
−5	3	18	2.54	2.54	218.1
−4	3	18	4.17	5.00	237.8
−3	3	18	5.54	5.37	248.6
−4	4	18	3.96	3.34	227.2
−3	2	20	1.57	1.75	299.2
2	2	20	2.52	2.96	204.8
−5	3	20	2.80	2.98	299.5
−4	3	20	2.81	2.67	270.7
−3	3	20	1.71	1.52	208.4
−6	4	20	1.90	1.83	275.6
−5	4	20	3.03	2.57	249.4
−4	4	20	3.52	2.64	206.3
−6	5	20	1.67	1.40	229.2
−5	5	20	2.47	2.26	198.8
1	1	21	1.88	1.69	261.1
−3	2	21	3.75	4.02	280.7
−2	2	21	2.17	2.13	348.3
2	2	21	3.91	4.63	248.1
−5	3	21	3.11	2.98	249.6
−4	3	21	3.68	4.14	286.3
−3	3	21	4.14	3.65	336.3
−5	4	21	2.10	2.35	276.5
−4	4	21	3.27	3.19	325.2
1	1	23	8.62	7.80	202.0
−3	2	23	4.49	4.04	299.9
−2	2	23	7.79	6.98	290.4
−5	3	23	2.28	2.34	144.1
−3	3	23	2.03	2.12	265.4
−5	4	23	2.24	2.21	122.1
−4	4	23	1.67	1.96	129.0
1	1	26	2.91	3.72	213.1
−3	2	26	4.25	4.10	347.3
−2	2	26	3.74	3.99	26.1
2	2	26	2.41	2.42	185.6
−4	3	26	2.22	2.25	341.9
−3	3	26	4.08	3.91	19.7
−4	4	26	1.33	1.76	353.0
−3	2	28	4.12	3.48	202.4
−2	2	28	2.98	3.28	166.5
2	2	28	2.28	2.43	335.0
−4	3	28	1.89	1.98	179.3
−3	3	28	3.53	3.13	158.5
−3	2	31	1.88	1.95	31.0
−3	2	33	0.95	1.29	92.9
2	2	33	1.83	1.3	126.5
−4	3	33	1.53	1.56	69.2
−3	3	33	1.41	1.68	41.7

Continued on the next page.

Continued.

h	*k*	*l*	|*Fo*|	|*Fc*|	*Phase*/°
0	1	0	75.54	70.81	0.0
−1	2	0	15.23	15.46	359.6
0	2	0	4.34	4.79	2.1
−1	3	0	7.41	6.87	181.6
0	3	0	8.81	8.33	184.4
−2	4	0	6.46	7.74	181.1
−1	4	0	5.86	6.93	183.3
0	4	0	4.24	4.42	187.9
−2	5	0	2.88	2.81	182.3
−1	5	0	1.60	1.34	187.8
1	1	1	3.72	2.97	161.9
−3	2	1	3.94	3.07	57.7
−2	2	1	3.65	3.97	10.3
2	2	1	2.60	2.12	191.2
−5	3	1	1.60	1.42	101.7
−4	3	1	0.73	1.24	77.3
−3	3	1	1.92	2.31	12.5
−5	4	1	1.32	1.16	100.9
−4	4	1	1.55	0.19	26.3
−1	1	2	1.04	1.11	258.8
1	1	2	0.84	0.51	201.2
−3	2	2	2.13	2.06	178.3
−2	2	2	1.24	1.29	224.5
2	2	2	2.73	2.97	101.5
−5	3	2	2.59	2.81	197.3
−4	3	2	3.36	3.19	165.1
−3	3	2	2.00	1.96	120.2
−5	4	2	2.84	2.24	154.1
−4	4	2	2.12	2.45	104.6
−1	1	3	2.44	2.48	247.0
1	1	3	6.39	6.24	156.0
−3	2	3	7.68	6.92	193.4
−2	2	3	6.69	6.86	243.3
2	2	3	4.84	5.15	157.3
−5	3	3	3.27	2.96	182.6
−4	3	3	5.21	5.55	209.0
−3	3	3	6.81	6.45	242.6
−5	4	3	2.23	2.76	217.5
−4	4	3	4.34	4.46	245.4
−1	1	4	2.67	2.67	25.4
1	1	4	7.69	6.93	46.1
−3	2	4	3.33	3.31	306.3
−2	2	4	6.99	6.42	321.1
−1	1	5	39.70	36.43	169.0
1	1	5	31.56	29.61	76.8
−3	2	5	11.28	10.77	180.3
−2	2	5	24.73	24.32	165.1
−5	3	5	3.30	3.14	14.9
−3	3	5	5.88	5.42	152.4
3	3	5	2.97	1.95	257.6
−5	4	5	3.14	3.11	354.9
−4	4	5	3.17	2.81	0.4
−5	5	5	4.04	2.36	342.9
−1	1	6	1.76	1.56	181.5
−2	2	6	2.39	2.73	201.2
−1	1	8	9.17	8.61	239.5
1	1	8	13.84	12.19	61.6
−3	2	8	10.68	9.57	204.1
−2	2	8	13.41	12.68	242.1
2	2	8	4.84	5.19	57.2
−4	3	8	4.39	4.70	210.3
−3	3	8	8.91	8.46	239.2
−1	1	9	9.71	9.36	282.2
1	1	9	3.51	3.84	282.4
−1	1	10	4.62	3.93	347.9
1	1	10	9.78	9.61	160.8
−3	2	10	10.44	9.86	15.5
−2	2	10	10.99	10.34	340.8
2	2	10	4.69	5.28	150.2
−4	3	10	4.16	4.41	355.8
−3	3	10	8.77	8.09	336.6
−1	1	13	15.56	13.63	230.7
1	1	13	14.37	13.67	318.8
−3	2	13	5.93	6.53	200.5
−2	2	13	12.89	11.66	225.9
−5	3	13	2.02	1.90	36.2
−3	3	13	2.69	2.95	207.1
−5	4	13	1.49	2.14	42.8
−4	4	13	2.21	2.07	58.4
−1	1	14	2.90	2.81	85.5
1	1	14	1.99	2.31	337.7
−2	2	14	1.84	1.96	63.7
−3	2	15	3.77	3.36	206.5
−2	2	15	2.10	2.18	158.0
2	2	15	2.70	3.17	238.2
−4	3	15	2.72	3.48	186.0
−3	3	15	4.70	4.04	156.0
−4	4	15	3.44	3.02	147.9
−1	1	18	12.76	12.27	212.5
1	1	18	4.09	4.45	198.9
−3	2	18	2.46	2.93	55.1
−2	2	18	3.44	1.82	176.1
2	2	18	3.75	3.35	40.3
−3	3	18	2.12	3.58	43.5
−3	2	21	2.09	1.88	42.7
2	2	21	1.83	2.08	18.4
−4	3	21	1.66	1.58	53.7
1	1	23	5.36	5.00	292.1
−3	2	23	2.65	2.62	24.3
−2	2	23	4.94	4.54	21.3
1	1	26	1.00	1.49	279.2
−3	2	26	2.08	1.66	63.3
−2	2	26	2.06	1.79	102.4
−3	3	26	1.69	1.82	96.1
−3	2	28	1.86	1.76	232.7
−2	2	28	1.75	1.72	200.3

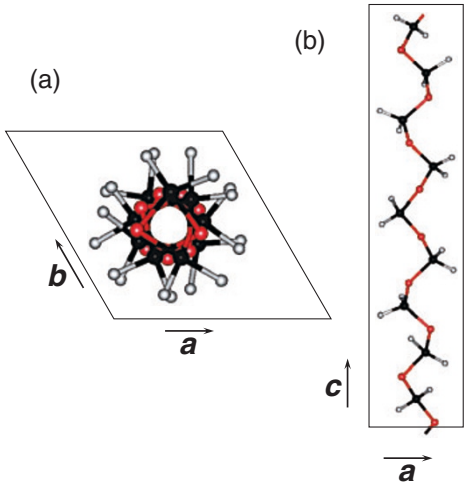

Figure 2. Crystal structure of polyxoymethylene (9/5) helical model analyzed at −150 °C on the basis of WAXD data measured with synchrotron X-ray beam of 0.3282 Å wavelength (Figure 1(a)).

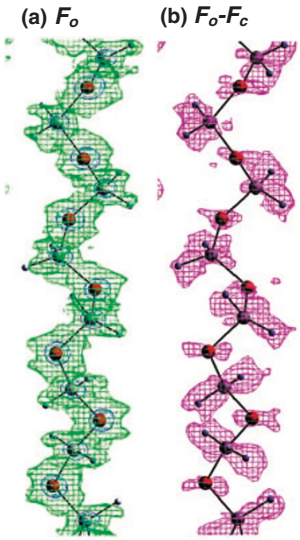

Figure 3. Fourier map (*Fo*) and difference Fourier (*Fo–Fc*) of polyoxymethylene crystal ((9/5) helical model) obtained on the basis of WAXD data at −150 °C.

Table III. Molecular Parameters of POM Chain Analyzed at (a) −150 °C and (b) Room Temperature (POM-h_2)

(a) −150 °C					
Bond Lengths/Å					
C(1)-O(2)	1.389(2)	O(2)-C(3)	1.429(3)	C(3)-O(4)	1.413(3)
O(4)-C(5)	1.406(2)	C(5)-O(6)	1.397(2)	O(6)-C(1**)	1.402(2)
C(1)-H(1)	0.96(3)	C(1)-H(2)	0.92(3)	C(3)-H(3)	0.94(5)
C(3)-H(4)	1.08(4)	C(5)-H(5)	0.97(3)	C(5)-H(6)	0.90(3)
Bond Angles/°					
C(1)-O(2)-C(3)	112.70(12)	O(4)-C(3)-O(2)	110.94(15)	C(5)-O(4)-C(3)	112.04(13)
O(4)-C(5)-O(6)	110.54(14)	O(2)-C(1)-O(6*)	110.77(14)	C(5*)-O(6*)-C(1)	114.52(12)
O(2)-C(1)-H(1)	112.3(17)	O(2)-C(1)-H(2)	111(2)	O(2)-C(3)-H(3)	102(2)
O(2)-C(3)-H(4)	107(4)	O(4)-C(3)-H(3)	122(3)	O(4)-C(3)-H(4)	101(3)
O(4)-C(5)-H(5)	112(2)	O(4)-C(5)-H(6)	112.8(19)	O(6)-C(5)-H(5)	110(2)
O(6)-C(5)-H(6)	111(2)	O(6*)-C(1)-H(1)	109(2)	O(6*)-C(1)-H(2)	114(2)
H(1)-C(1)-H(2)	100(3)	H(3)-C(3)-H(4)	112(3)	H(5)-C(5)-H(6)	100(3)
Torsion Angles/°					
C(1)-O(2)-C(3)-O(4)	77.6(5)	O(2)-C(3)-O(4)-C(5)	78.8(5)	C(3)-O(4)-C(5)-O(6)	79.2(5)
O(4)-C(5)-O(6)-C(1*)	76.6(5)	O(6*)-C(1)-O(2)-C(3)	79.3(5)	C(5*)-O(6*)-C(1)-O(2)	75.7(5)
(b) 20 °C					
Bond Lengths/Å					
C(1)-O(2)	1.441(13)	O(2)-C(3)	1.341(13)	C(3)-O(4)	1.433(13)
O(4)-C(5)	1.353(13)	C(5)-O(6)	1.422(14)	O(6)-C(1**)	1.369(13)
C(1)-H(1)	1.05(7)	C(1)-H(2)	1.01(7)	C(3)-H(3)	1.08(11)
C(3)-H(4)	0.83(7)	C(5)-H(5)	0.96(8)	C(5)-H(6)	1.14(9)
Bond Angles/°					
C(1)-O(2)-C(3)	115.3(8)	O(4)-C(3)-O(2)	112.1(8)	C(5)-O(4)-C(3)	116.4(7)
O(4)-C(5)-O(6)	110.2(8)	O(2)-C(1)-O(6*)	110.3(7)	C(5*)-O(6*)-C(1)	114.1(7)
O(2)-C(1)-H(1)	105(3)	O(2)-C(1)-H(2)	107(6)	O(2)-C(3)-H(3)	117(7)
O(2)-C(3)-H(4)	114(6)	O(4)-C(3)-H(3)	101(6)	O(4)-C(3)-H(4)	109(7)
O(4)-C(5)-H(5)	105(6)	O(4)-C(5)-H(6)	113(6)	O(6)-C(5)-H(5)	107(6)
O(6)-C(5)-H(6)	106(5)	O(6*)-C(1)-H(1)	119(4)	O(6*)-C(1)-H(2)	109(5)
H(1)-C(1)-H(2)	106(5)	H(3)-C(3)-H(4)	103(7)	H(5)-C(5)-H(6)	116(8)
Torsion Angles/°					
C(1)-O(2)-C(3)-O(4)	75.7(10)	O(2)-C(3)-O(4)-C(5)	81.1(9)	C(3)-O(4)-C(5)-O(6)	75.1(10)
O(4)-C(5)-O(6)-C(1*)	84.5(10)	O(6*)-C(1)-O(2)-C(3)	83.2(9)	C(5*)-O(6*)-C(1)-O(2)	76.1(10)

Table IV. Averaged Molecular Parameters of POM (9/5) Chain Analyzed by WAXD and WAND

	WAXD (9/5) (POM-h_2, −150 °C)	WAXD (9/5) (POM-h_2, 20°C)	WAND (9/5, POM-h_2)	WAND (9/5, POM-d_2)	WAXD (29/16, POM-h_2, −150 °C)
Bond Lengths/Å					
C-O	1.406	1.393	—	—	1.410
C-H	0.962	1.130	1.040	1.060	(0.970)
Bond Angles/°					
C-O-C	113.1	115.2	115.2	115.2	113.5
O-C-O	110.8	110.9	110.9	110.9	111.5
O-C-H	110.3	110.0	111.0	108.0	110.5
H-C-H	104.0	103.0	105.0	111.0	108.7
Torsional Angles/°					
C-O-C-O	77.9	79.9	79.9	79.9	78.1

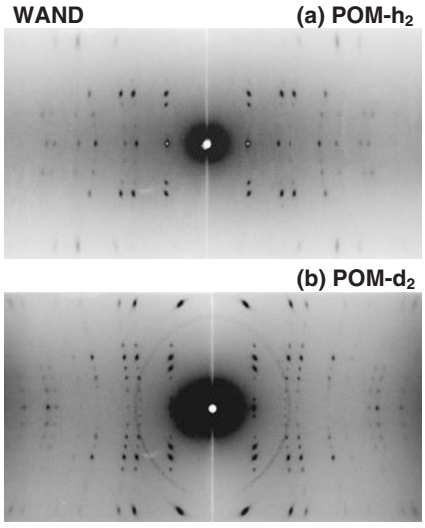

Figure 4. Full-rotation neutron diffraction diagrams of solid-state-polymerized polyoxymethylene samples measured at room temperature. (a) Hydrogenated POM (POM-h_2) and (b) deuterated POM (POM-d_2). The vertical direction is parallel to the *c* axis.

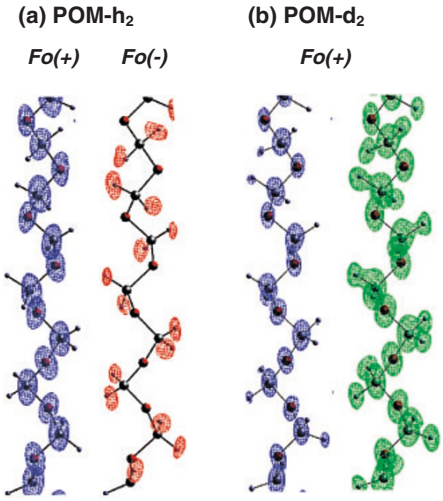

Figure 5. Fourier map (*Fo*) of polyoxymethylene crystal ((9/5) helical model) obtained on the basis of WAND data at room temperature: (a) POM-h_2 and (b) POM-d_2. *Fo*(+) and *Fo*(−) indicate the density distributions of atomic nuclei in the region of positive and negative density height, respectively. In case of POM-d_2, the left and right figures show the density distribution in the higher and lower height region, respectively.

difference Fourier synthesis (*Fo–Fc*). The hydrogen atoms are clearly detected in the *Fo–Fc* map. Table III(a) and III(b) show the various molecular parameters evaluated at −150 °C and room temperature, respectively. The standard errors are appreciably smaller than the previously reported values.[4] It should be noticed here that the present X-ray data allowed us to refine the hydrogen atomic positions, different from the previous analysis in which the hydrogen atomic positions could not be refined but were fixed to the standard geometrical values.[4] Table IV summarizes the averaged values and their dispersions obtained by the present analysis. As seen in this table, the averaged geometry is reasonable as a whole, although the molecular parameters do not take the common values necessarily but distribute to some extent. For example, the skeletal torsional angles distribute from 75.7° to 79.3° for COCO and OCOC segments.

Structure Analysis using WAND Data

Figure 4(a) and 4(b) show, respectively, the full-rotation WAND diagrams taken for POM-h_2 and POM-d_2 at room temperature. POM-h_2 sample gave clearer reflections than expected for the hydrogenated species. The WAND pattern of POM-d_2 is appreciably different from that of POM-h_2. The background scattering is clearer for POM-d_2, since the incoherent background is reduced drastically because of larger contribution of coherent neutron scattering from deuterium. The total number of reflections observed for POM-h_2 is 130. It is 244 for POM-d_2. The number of unique reflections used in the least squares refinement was 25 for POM-h_2 and 57 for POM-d_2. The chain structure obtained by the X-ray structure analysis at room temperature was transferred to the struc-

Table V. Atomic Fractional Coordinates and Thermal Parameters of POM-h_2 and POM-d_2 Analyzed by WAND Data (Room Temperature)

(a) POM-h_2

Atom	x/a	y/b	z/c	U_{iso}/Å^2
C(1)	1.0936	0.1792	−0.1891	0.100(4)
O(2)	0.8433	−0.0435	−0.133	0.104(5)
C(3)	0.9659	−0.1657	−0.0783	0.087(3)
O(4)	1.1658	0.0917	−0.0219	0.096(5)
C(5)	0.9857	0.1446	0.0339	0.087(4)
O(6)	0.8545	−0.1315	0.0879	0.103(5)
H(1)	1.022(4)	0.373(5)	−0.207(2)	0.113(7)
H(2)	1.322(6)	0.332(5)	−0.157(3)	0.116(7)
H(3)	1.147(4)	−0.244(4)	−0.0986(15)	0.097(7)
H(4)	0.804(4)	−0.357(4)	−0.0537(14)	0.101(6)
H(5)	1.148(4)	0.352(4)	0.0576(19)	0.116(8)
H(6)	0.750(4)	0.160(4)	0.011(2)	0.110(8)

Atom	U_{11}	U_{22}	U_{33}	U_{23}	U_{13}	U_{12}/Å^2
C(1)	0.106(5)	0.076(4)	0.110(10)	0.006(6)	−0.002(5)	0.038(4)
O(2)	0.093(4)	0.117(5)	0.102(13)	−0.004(6)	−0.001(6)	0.052(4)
C(3)	0.101(4)	0.079(4)	0.095(8)	0.001(5)	−0.007(4)	0.055(3)
O(4)	0.096(4)	0.097(5)	0.090(14)	−0.009(6)	0.002(6)	0.044(4)
C(5)	0.094(3)	0.079(3)	0.126(11)	0.002(4)	0.004(5)	0.071(3)
O(6)	0.087(5)	0.085(5)	0.125(13)	−0.002(7)	0.006(7)	0.034(5)
C(1)	0.117(11)	0.101(9)	0.110(12)	−0.008(10)	−0.002(10)	0.046(7)
O(2)	0.109(10)	0.097(10)	0.116(13)	0.007(13)	0.000(11)	0.032(8)
C(3)	0.087(7)	0.091(7)	0.126(17)	0.013(9)	0.009(10)	0.055(6)
O(4)	0.093(6)	0.093(7)	0.135(16)	−0.029(10)	0.014(8)	0.060(6)
C(5)	0.094(6)	0.094(8)	0.19(2)	0.029(10)	−0.025(11)	0.067(6)
O(6)	0.099(6)	0.082(7)	0.19(2)	−0.022(10)	−0.008(10)	0.076(5)

(b) POM-d_2

Atom	x/a	y/b	z/c	U_{iso}/Å^2
C(1)	1.0936	0.1792	−0.1891	0.076(4)
O(2)	0.8433	−0.0435	−0.133	0.074(4)
C(3)	0.9659	−0.1657	−0.0783	0.078(4)
O(4)	1.1658	0.0917	−0.0219	0.075(5)
C(5)	0.9857	0.1446	0.0339	0.077(4)
O(6)	0.8545	−0.1315	0.0879	0.066(5)
H(1)	1.007(3)	0.350(3)	−0.208(2)	0.117(6)
H(2)	1.328(3)	0.322(3)	−0.153(2)	0.128(7)
H(3)	1.144(2)	−0.234(2)	−0.0974(17)	0.103(6)
H(4)	0.807(3)	−0.357(3)	−0.049(2)	0.143(8)
H(5)	1.160(3)	0.359(2)	0.0657(17)	0.118(9)
H(6)	0.753(2)	0.146(2)	0.0025(19)	0.148(10)

Atom	U_{11}	U_{22}	U_{33}	U_{23}	U_{13}	U_{12}/Å^2
C(1)	0.084(2)	0.086(2)	0.089(13)	0.000(5)	−0.007(5)	0.0665(17)
O(2)	0.083(3)	0.090(4)	0.064(12)	0.004(6)	−0.020(7)	0.056(2)
C(3)	0.098(3)	0.083(3)	0.069(11)	0.012(6)	0.002(6)	0.057(2)
O(4)	0.091(3)	0.083(3)	0.066(13)	0.010(6)	−0.001(7)	0.055(2)
C(5)	0.090(3)	0.086(3)	0.073(11)	0.006(5)	−0.008(6)	0.058(2)
O(6)	0.092(3)	0.075(3)	0.047(14)	−0.007(6)	−0.009(7)	0.053(2)
C(1)	0.129(5)	0.115(5)	0.089(16)	−0.011(9)	−0.009(9)	0.046(4)
O(2)	0.107(5)	0.119(6)	0.099(17)	0.000(9)	−0.029(9)	0.011(5)
C(3)	0.096(3)	0.099(4)	0.126(16)	−0.001(7)	−0.012(7)	0.059(3)
O(4)	0.137(7)	0.107(7)	0.124(18)	0.006(9)	−0.034(12)	0.015(6)
C(5)	0.127(6)	0.091(4)	0.12(3)	−0.003(8)	−0.015(11)	0.041(4)
O(6)	0.099(4)	0.108(4)	0.25(3)	−0.007(10)	0.005(9)	0.063(3)

Table VI. Molecular Parameters Obtained by the WAND Data of Hydrogenated POM (POM-h_2) and Deuterated POM (POM-d_2) at Room Temperature

(a) POM-h_2					
Bond Lengths/Å					
C(1)-O(2)	1.389	O(2)-C(3)	1.429	C(3)-O(4)	1.413
O(4)-C(5)	1.406	C(5)-O(6)	1.397	O(6)-C(1**)	1.402
C(1)-H(1)	1.117(18)	C(1)-H(2)	0.914(11)	C(3)-H(3)	0.96(2)
C(3)-H(4)	1.11(2)	C(5)-H(5)	1.037(15)	C(5)-H(6)	0.91(2)
Bond Angles/°					
C(1)-O(2)-C(3)	112.70	O(4)-C(3)-O(2)	110.94	C(5)-O(4)-C(3)	112.04
O(4)-C(5)-O(6)	110.54	O(2)-C(1)-O(6*)	110.77	C(5*)-O(6*)-C(1)	114.52
O(2)-C(1)-H(1)	107.6(15)	O(2)-C(1)-H(2)	105.0(30)	O(2)-C(3)-H(3)	114.9(13)
O(2)-C(3)-H(4)	115.1(13)	O(4)-C(3)-H(3)	102.3(10)	O(4)-C(3)-H(4)	108.4(15)
O(4)-C(5)-H(5)	104.6(16)	O(4)-C(5)-H(6)	113.8(16)	O(6)-C(5)-H(5)	110.2(17)
O(6)-C(5)-H(6)	106.5(12)	O(6*)-C(1)-H(1)	118.0(20)	O(6*)-C(1)-H(2)	114.0(20)
H(1)-C(1)-H(2)	101.8(18)	H(3)-C(3)-H(4)	102.8(15)	H(5)-C(5)-H(6)	111.7(14)
Torsion Angles/°					
C(1)-O(2)-C(3)-O(4)	77.6	O(2)-C(3)-O(4)-C(5)	78.8	C(3)-O(4)-C(5)-O(6)	79.2
O(4)-C(5)-O(6)-C(1*)	76.6	O(6*)-C(1)-O(2)-C(3)	79.3	C(5*)-O(6*)-C(1)-O(2)	75.7
(b) POM-d_2					
Bond Lengths/Å					
C(1)-O(2)	1.389	O(2)-C(3)	1.429	C(3)-O(4)	1.413
O(4)-C(5)	1.406	C(5)-O(6)	1.397(2)	O(6)-C(1**)	1.402
C(1)-H(1)	1.064(19)	C(1)-H(2)	1.110(20)	C(3)-H(3)	1.038(14)
C(3)-H(4)	0.940(20)	C(5)-H(5)	1.042(17)	C(5)-H(6)	1.177(18)
Bond Angles/°					
C(1)-O(2)-C(3)	112.70	O(4)-C(3)-O(2)	110.94	C(5)-O(4)-C(3)	112.04
O(4)-C(5)-O(6)	110.54	O(2)-C(1)-O(6*)	110.77	C(5*)-O(6*)-C(1)	114.52
O(2)-C(1)-H(1)	105.8(14)	O(2)-C(1)-H(2)	101.2(15)	O(2)-C(3)-H(3)	114.9(15)
O(2)-C(3)-H(4)	118.7(13)	O(4)-C(3)-H(3)	101.1(11)	O(4)-C(3)-H(4)	103.7(18)
O(4)-C(5)-H(5)	107.7(11)	O(4)-C(5)-H(6)	105.7(14)	O(6)-C(5)-H(5)	104.0(13)
O(6)-C(5)-H(6)	109.3(9)	O(6*)-C(1)-H(1)	115.0(2)	O(6*)-C(1)-H(2)	109.1(8)
H(1)-C(1)-H(2)	105.8(10)	H(3)-C(3)-H(4)	110.1(16)	H(5)-C(5)-H(6)	112.9(12)
Torsion Angles/°					
C(1)-O(2)-C(3)-O(4)	77.6	O(2)-C(3)-O(4)-C(5)	78.8	C(3)-O(4)-C(5)-O(6)	79.2
O(4)-C(5)-O(6)-C(1*)	76.6	O(6*)-C(1)-O(2)-C(3)	79.3	C(5*)-O(6*)-C(1)-O(2)	75.7

ture refinement based on the WAND data. The final reliability factor was 13.9% for WAND-h_2 data and 22.4% for WAND-d_2 data, where the coordinates of C and O atoms were fixed and such parameters were refined as the anisotropic thermal parameters of C and O atoms and the positions and anisotropic temperature parameters for H atoms. The finally-obtained atomic coordinates are shown in Table V. The molecular parameters are listed in Table VI. The hydrogen atoms detected in the *Fo* map are shown in Figure 5(a) and 5(b) for POM-h_2 and POM-d_2, respectively. As seen in Table VI, the molecular parameters associated with the H atoms are C-H = 1.04 Å and H-C-H angle = 105.0° for POM-h_2 and 1.06 Å and 111.0° for POM-d_2, which are reasonable and in good

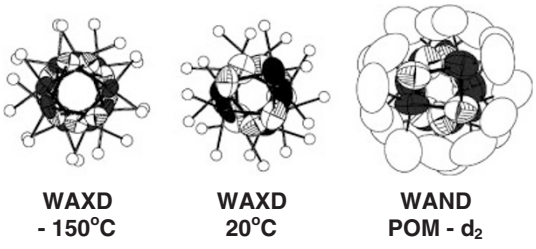

Figure 6. Atomic thermal parameters of POM chain ((9/5) helical model) analyzed with WAXD data (−150 °C and room temperature) and WAND data (room temperature). In the X-ray data analysis the isotropic thermal parameters were assumed for hydrogen atoms, while the anisotropic thermal parameters in the neutron data analysis.

agreement with the WAXD results within the experimental errors.

The anisotropic thermal parameters are compared between the structures obtained at −150 °C and room temperature. As shown in Figure 6, the skeletal C and O atoms show the anisotropic thermal motion with small amplitude at −150 °C. The WAND result shows that the anisotropic thermal parameters, especially those of H (D) atoms are larger along the circular direction of the cross section of the helix at room temperature. This makes us speculate that the molecular chains experience the librational motion around the chain axis and it becomes more active at room temperature. This is consistent with the already reported papers using the X-ray diffraction method and the solid-state NMR method.[25,26]

Structural Analysis Based on (29/16) Helical Model (1) Discussion Using the WAXD Data

In the preceding sections we analyzed the WAXD and WAND data on the basis of non-uniform (9/5) helical chain conformation, where the *c*-axial length corresponding to this conformational model was used and estimated as an average of the interlayer spacings (for example, the 9.7-th layer line estimated from the interlayer spacing was assumed to be the 10th layer line). In a similar way with that reported by Carazzolo,[17] more exact fiber period was evaluated by investigating the interlayer spacings for all the layer lines up to 33rd layer line in more accurate way. Strictly speaking, the fiber period 17.274 Å is not exact, which was used in the analysis of (9/5) helical model at −150 °C, but it should be 55.710 Å so that all the layer lines are assigned to almost perfect integers. As shown in Figure 7(b), we found for the first time the existence of strong meridional reflections at quite low diffraction angles in the full-rotation X-ray diagram taken at room temperature for γ-ray-polymerized POM sample, corresponding to the lattice spacings of about 56.0 and 28.0 Å or the 001 and 002 reflections of the repeating period 56.0 Å. In this way we have been able to confirm the repeating period along the *c* axis (56.0 Å at room temperature and 55.7 Å at −150 °C). As shown in Figure 7(a), we have measured the *00l* reflections by the Norman's method, *i.e.*, the sample was oscillated around the axis perpendicular to the *c* axis. In addition to the strong 0029 reflection (corresponding to 009 of (9/5) model) and 0058 reflection (0018), there observed many reflections which cannot be interpreted at all on the basis of (9/5) helix. They can be indexed reasonably by the (29/16) model. In this way, Figure 7 has allowed us to confirm the existence of molecular chain with 56 Å repeating period. Using the 85 X-ray reflections collected by an automatic four-circle diffractometer with Mo-Kα X-ray beam, Takahashi and Tadokoro performed the structural refinement of *uniform* (29/16) helix.[27] But we do not need to assume such a uniform helical structure for the structure analysis. Under the assumption of space group symmetry *P*1, which should be reasonable since a series of the observed *00l* reflections can not be explained by 3_2 screw symmetry, we applied the direct method to the unit cell of $c = 55.710$ Å using the 184 unique reflections collected at −150 °C. The direct method was found to give the (29/16) model straightforwardly with the reliability factor 19.3%. The structural refinement was performed for the atomic coordinates and isotropic thermal parameters of C and O atoms. The hydrogen atoms could be extracted by performing the *Fo–Fc* synthesis as shown in Figure 8(b). The positions of hydrogen atoms were tried to refine, but they did not give reasonable geometry concerning C-H bond length and H-C-H bond angle. Then the hydrogen atoms were added to the (29/16) chain using the standard geometry. The structure after the refinement gave the reliability factor 8.6%. The molecular chain conformation is shown in Figure 8(a). Tables VII and VIII show the fractional coordinates of atoms and the comparison between *Fo* and *Fc*, respectively. As shown in Table IV, the molecular parameters are not yet satisfactory from the stereochemical point of view, because the reasonable structure refinement could not be made enough well due to too small number of observed reflections (184) compared with the total number of adjustable parameters (4 parameters × 29 monomeric units × 2 atoms (C and O)/monomeric unit + scale factor = 224 parameters if isotropic thermal parameters are assumed).

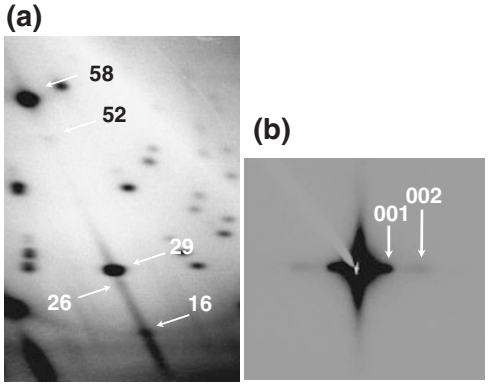

Figure 7. X-Ray meridional *00l* reflections measured for POM-h_2 sample by (a) the Norman's method using a Weissenberg camera with the sample oscillation around the axis perpendicular to the *c* axis and (b) the full rotation method around the *c* axis. In (b), the *c* axis is along the horizontal line. The strong streak line along the vertical direction is due to the void scattering.

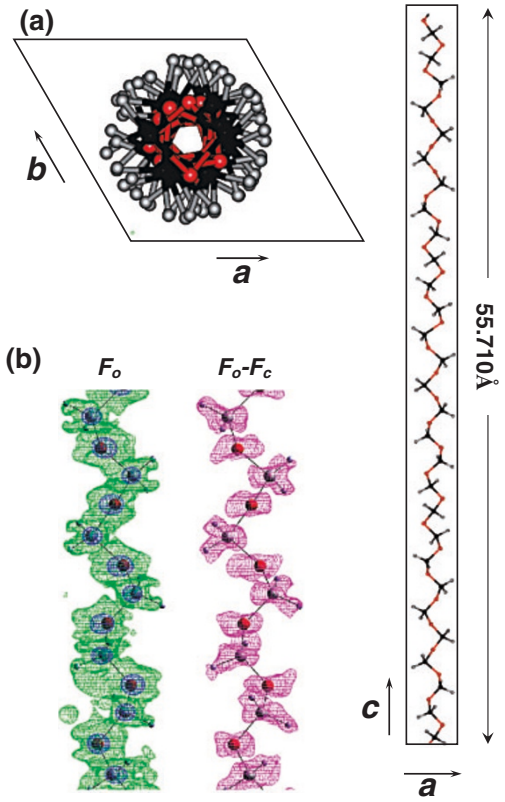

Figure 8. (a) Refined crystal structure and (b) Fourier maps (*Fo* and *Fo–Fc*) obtained for polyoxymethylene (29/16) helical model using a WAXD data measured at −150 °C (refer to Figure 1(a)).

(2) Discussion Using the WAND Data

It is valuable to check the reasonableness of the thus refined (29/16) helical model on the basis of WAND data. But the WAND data were collected at room temperature, and it is impossible to transfer the above-mentioned structural information which was obtained using the WAXD data at −150 °C. Besides the total number of neutron reflections observed at room temperature is quite limited, and so the full refinement of the complicated (29/16) helical model is not possible. Then, we analyzed at first the WAXD data taken at room temperature starting from the atomic coordinates determined at −150 °C, and the thus obtained information was applied to the analysis of WAND data. In the structure analysis of WAXD data collected at room temperature, the least-squares refinement was performed by utilizing the positions and isotropic thermal parameters of C and O atoms as the adjustable parameters since the total number of X-ray reflections at room temperature is only 428, not enough for the full refinement of the nonuniform (29/16) helical structure. The hydrogen atoms were added to the standard positions after the structure analysis for C and O atoms only. The final reliability factor was 10.7%. The thus-obtained structure model was transferred to the WAND data treatment. At first the WAND data taken for POM-h_2 sample was used and only the positions and isothermal parameters of hydrogen atoms were refined with the coordinates and thermal parameters of C and O atoms fixed at the X-ray-determined values. The structural refinement was failed: the reliability factor was 30.2%. The total number of neutron reflections observed for POM-h_2 sample was only 130, among which the unique reflections were only 25, making it impossible to perform the refinement of nonuniform (29/16) helix model even if the C and O atomic positions were fixed to the X-ray determined ones. As the next trial, the refinement was made successfully for the WAND data measured for POM-d_2 sample, where the 244 reflections were obtained in total and the 57 reflections were unique. The atomic coordinates and isotropic thermal parameters of D atoms were refined with the parameters concerning C and O atoms fixed to the X-ray analyzed values. The reliability factor was 11.2%. The thus-obtained atomic coordinates and thermal parameters of the nonuniform (29/16) helical model are listed in Table IX.

In this way both of the WAXD and WAND data are not inconsistent with the nonuniform (29/16) helical model both at −150 °C and at room temperature. But, as mentioned before, the (9/5) helical model can give us also good agreements between the observed and calculated data of WAXD and WAND at almost the same level of accuracy. In other words, it is difficult at present to judge which model is more reasonable between the nonuniform (9/5) helix and the nonuniform (29/16) helix as long as the reliability factor is compared. In particular as for the X-ray diffraction data taken at −150 °C, these two models give very good agreements between the observed and calculated intensities at a high level comparable to the case of single crystals of low-molecular-weight compounds. The similar thing can be said also to the neutron cases though the reliability factors are not very low compared with the X-ray cases. In this way we cannot distinguish the superiority of the models only through the comparison in structure factors collected from the full-rotation X-ray (and neutron) diffraction patterns even though they gave more than 700 reflections! Luckily we have several experimental evidences which can support the nonuniform (29/16) helical model as the most plausible one. These experimental evidences were already shown in Figure 7: (i) the repeating period along the *c* axis should be 55.71 Å, and (ii) the *00l* reflections do not satisfy the extinction rules requested from the uniform (9/5) helix (*00l*, $l = 9, 18, \ldots$) or 3/1 helix symmetry (00*l*, $l = 3, 6, 9, \ldots$). In fact the *00l* reflections calculated using the atomic coordinates given in Table VII are in good agreement

Table VII. Atomic Coordinated and Thermal parameters of POM (29/16) Helical Model Derived from WAXD Data at −150 °C

Atom	x/a	y/b	z/c	U_{iso}/Å^2	Atom	x/a	y/b	z/c	U_{iso}/Å^2
O01	1.0726(14)	0.7091(13)	−0.00136(13)	0.0254(13)	H01	1.1523	0.3263	0.0083	0.049(3)
C02	1.1289(16)	0.5112(18)	0.01623(16)	0.0185(12)	H02	1.3500	0.6643	0.0244	0.049(3)
O03	0.8643(10)	0.3594(10)	0.03310(10)	0.0157(8)	H03	0.6508	0.5027	0.0585	0.050(3)
C04	0.8797(11)	0.5925(11)	0.05088(10)	0.0104(8)	H04	0.9500	0.8222	0.0440	0.050(3)
O05	1.1386(11)	0.6190(12)	0.06820(10)	0.0154(8)	H05	1.1957	0.3934	0.0932	0.049(3)
C06	1.0030(20)	0.4000(20)	0.0851(2)	0.0251(16)	H06	0.861	0.1699	0.0777	0.050(3)
O07	0.8003(11)	0.4247(12)	0.10242(11)	0.0168(9)	H07	0.7986	0.7356	0.1283	0.049(3)
C08	0.9680(20)	0.694(2)	0.11983(19)	0.0283(18)	H08	1.1464	0.9129	0.1126	0.049(3)
O09	1.1356(17)	0.5376(19)	0.13667(16)	0.0295(16)	H09	1.0547	0.2489	0.1626	0.050(3)
C10	0.9392(15)	0.3554(16)	0.15394(12)	0.0139(10)	H10	0.7192	0.1663	0.1475	0.050(3)
O11	0.8591(17)	0.5737(19)	0.17117(15)	0.0274(14)	H11	1.3475	0.7720	0.1800	0.050(3)
C12	1.1260(18)	0.7012(18)	0.18815(14)	0.0172(12)	H12	1.1433	0.9114	0.1953	0.049(3)
O13	1.0886(12)	0.4750(12)	0.20596(10)	0.0144(9)	H13	0.8334	0.1799	0.2314	0.050(3)
C14	0.8490(20)	0.382(20)	0.22303(19)	0.0236(17)	H14	0.6218	0.304	0.2155	0.049(3)
O15	0.9030(15)	0.6393(16)	0.24017(13)	0.0201(11)	H15	1.3374	0.6273	0.2495	0.049(3)
C16	1.1569(17)	0.6541(18)	0.25775(14)	0.0161(12)	H16	1.2712	0.8847	0.2653	0.050(3)
O17	1.0069(17)	0.3984(17)	0.27528(14)	0.0242(14)	H17	0.6686	0.5700	0.2832	0.050(3)
C18	0.7927(17)	0.4730(19)	0.29195(14)	0.0153(11)	H18	0.6190	0.2562	0.2997	0.050(3)
O19	1.0140(20)	0.7160(20)	0.30938(17)	0.0324(19)	H19	1.1742	0.3524	0.3178	0.049(3)
C20	1.1380(20)	0.5250(20)	0.32638(17)	0.0179(15)	H20	1.3549	0.6901	0.3345	0.049(3)
O21	0.8451(14)	0.3531(14)	0.34338(12)	0.0174(11)	H21	0.8578	0.7903	0.3529	0.050(3)
C22	0.8240(30)	0.5760(30)	0.3606(2)	0.0290(20)	H22	0.5914	0.4591	0.3680	0.049(3)
O23	1.0779(15)	0.6604(15)	0.37794(11)	0.0163(10)	H23	0.9104	0.169	0.387	0.050(3)
C24	1.0194(17)	0.3963(17)	0.39503(12)	0.0113(11)	H24	1.2455	0.442	0.4013	0.050(3)
O25	0.8182(16)	0.3791(16)	0.41310(13)	0.0196(13)	H25	1.0950	0.8613	0.4215	0.050(3)
C26	0.9520(30)	0.6380(20)	0.42965(19)	0.0216(16)	H26	0.7575	0.6475	0.4373	0.049(3)
O27	1.1552(18)	0.6030(20)	0.44734(16)	0.0255(16)	H27	0.7864	0.1564	0.4567	0.049(3)
C28	0.9710(20)	0.3670(20)	0.46439(18)	0.0183(15)	H28	1.1269	0.3019	0.4724	0.049(3)
O29	0.8226(18)	0.4684(19)	0.48090(14)	0.0258(15)	H29	1.2898	0.8597	0.4917	0.050(3)
C30	1.0622(18)	0.6989(16)	0.49882(12)	0.0116(10)	H30	0.9698	0.8362	0.5063	0.050(3)
O31	1.0950(20)	0.4790(20)	0.51583(18)	0.0270(17)	H31	0.5875	0.2997	0.5253	0.049(3)
C32	0.8050(20)	0.3500(20)	0.53316(16)	0.0166(14)	H32	0.7707	0.1361	0.5409	0.049(3)
O33	0.9073(15)	0.6274(16)	0.55043(12)	0.0151(11)	H33	1.1680	0.9037	0.5772	0.050(3)
C34	1.1340(20)	0.6980(20)	0.56829(16)	0.0202(16)	H34	1.3610	0.7456	0.5621	0.049(3)
O35	0.9746(17)	0.3671(17)	0.58497(13)	0.0167(12)	H35	0.6487	0.2025	0.6103	0.050(3)
C36	0.8071(19)	0.426(2)	0.60263(15)	0.0143(13)	H36	0.6632	0.5151	0.5957	0.050(3)
O37	1.0220(20)	0.6629(19)	0.62028(15)	0.0254(15)	H37	1.2984	0.8208	0.6448	0.050(3)
C38	1.1491(19)	0.6000(20)	0.63643(14)	0.0140(13)	H38	1.3029	0.5197	0.6300	0.049(3)
O39	0.9226(18)	0.3448(18)	0.65417(15)	0.0214(15)	H39	0.6375	0.3324	0.6797	0.049(3)
C40	0.8440(20)	0.5080(20)	0.67108(15)	0.0182(14)	H40	0.7804	0.6671	0.6634	0.049(3)
O41	1.1207(18)	0.7062(18)	0.68824(15)	0.0191(14)	H41	1.3264	0.5715	0.7147	0.050(3)
C42	1.1030(20)	0.4730(20)	0.70615(17)	0.0174(16)	H42	1.0521	0.2493	0.6991	0.050(3)
O43	0.8076(17)	0.4202(18)	0.72333(13)	0.0223(13)	H43	0.7704	0.7212	0.7476	0.049(3)
C44	0.9590(20)	0.6990(20)	0.74013(15)	0.0169(13)	H44	1.1078	0.9169	0.7315	0.050(3)
O45	1.1545(16)	0.6650(17)	0.75777(13)	0.0166(13)	H45	0.7957	0.1506	0.7670	0.049(3)
C46	0.9680(50)	0.3640(50)	0.7751(4)	0.0400(30)	H46	1.1346	0.3171	0.7836	0.049(3)
O47	0.7956(15)	0.4948(17)	0.79169(12)	0.0165(12)	H47	1.2240	0.8942	0.8018	0.049(3)
C48	1.0190(20)	0.7020(20)	0.80947(14)	0.0117(12)	H48	0.9007	0.8060	0.8181	0.049(3)
O49	1.1360(20)	0.5600(20)	0.82577(19)	0.0280(20)	H49	0.6387	0.2149	0.8349	0.050(3)
C50	0.8620(20)	0.3490(20)	0.84333(16)	0.0154(15)	H50	0.9176	0.1822	0.8507	0.050(3)
O51	0.8192(14)	0.5430(15)	0.86129(10)	0.0121(9)	H51	1.3672	0.7292	0.8687	0.049(3)
C52	1.1630(30)	0.695(30)	0.8778(2)	0.0270(20)	H52	1.2153	0.9158	0.8853	0.050(3)
O53	1.0582(15)	0.4181(15)	0.89525(11)	0.0123(10)	H53	0.7047	0.1503	0.9212	0.050(3)
C54	0.7920(30)	0.373(30)	0.91280(19)	0.0187(18)	H54	0.5954	0.3753	0.9050	0.049(3)
O55	0.9760(20)	0.6810(20)	0.93013(16)	0.0192(16)	H55	1.2347	0.4207	0.9388	0.050(3)
C56	1.1509(19)	0.5600(20)	0.94716(14)	0.0143(13)	H56	1.3515	0.7603	0.9546	0.049(3)
O57	0.8973(16)	0.3497(15)	0.96497(11)	0.0135(10)	H57	0.7904	0.7194	0.9732	0.049(3)
C58	0.8220(20)	0.544(30)	0.98178(18)	0.0223(19)	H58	0.6011	0.3854	0.9897	0.049(3)

Table VIII. Comparison of Observed and Calculated Structure Factor for POM (29/16) Helix Model at −150 °C (POM-h_2)

h	*k*	*l*	*|Fo|*	*|Fc|*	*Phase/°*	*h*	*k*	*l*	*|Fo|*	*|Fc|*	*Phase/°*
1	0	0	227.24	226.85	193.7	1	1	16	105.78	104.85	347.0
2	0	0	11.43	12.18	43.4	2	1	16	39.74	40.50	191.7
3	0	0	34.36	36.21	38.3	4	1	16	15.00	14.96	52.9
4	0	0	19.33	18.91	239.8	5	1	16	5.78	5.85	263.8
5	0	0	4.23	4.09	213.7	3	2	16	11.28	15.09	101.2
6	0	0	12.38	8.10	81.2	4	2	16	9.21	8.94	306.9
1	1	0	46.8	48.72	87.7	3	3	16	8.62	10.22	350.0
2	1	0	28.2	28.97	101.9	1	0	19	4.37	6.10	327.5
3	1	0	26.92	29.20	297.9	2	0	19	9.92	9.51	134.2
4	1	0	5.33	5.39	151.8	3	0	19	8.42	6.47	321.3
5	1	0	7.14	7.63	139.9	1	1	19	3.18	2.99	124.3
2	2	0	27.95	32.22	0.6	2	1	19	3.89	4.05	353.6
3	2	0	12.83	12.37	199.5	4	0	22	7.11	6.74	347.0
4	2	0	4.09	4.44	196.6	5	0	22	7.74	8.34	179.6
5	2	0	3.64	6.15	46.4	6	0	22	9.84	6.71	14.1
3	3	0	3.53	2.56	263.5	3	1	22	6.60	6.64	326.3
4	3	0	7.03	5.90	105.6	4	1	22	10.02	8.80	181.9
2	0	3	15.1	13.43	217.1	5	1	22	6.63	7.44	30.8
3	0	3	8.95	8.11	49.7	3	2	22	10.19	10.13	189.2
1	1	3	12.45	10.37	195.0	4	2	22	7.99	8.56	41.8
2	1	3	13.36	12.18	46.1	3	3	22	5.51	8.74	57.6
3	1	3	5.59	5.04	222.7	4	3	22	5.65	5.63	270.3
2	2	3	7.75	7.70	257.4	1	0	26	33.68	30.58	42.1
3	0	6	13.16	15.00	226.3	2	0	26	49.90	48.08	234.3
4	0	6	18.07	18.32	57.6	3	0	26	35.39	35.99	69.5
5	0	6	14.36	13.33	253.8	4	0	26	13.54	12.36	273.3
2	1	6	10.27	11.49	210.9	6	0	26	8.75	6.05	116.5
3	1	6	16.30	18.34	69.2	1	1	26	52.69	47.55	1.4
4	1	6	15.96	16.12	274.6	2	1	26	43.33	41.30	170.5
5	1	6	7.33	8.79	118.8	3	1	26	19.14	21.28	354
2	2	6	13.60	17.07	70.4	4	1	26	4.91	1.24	258.6
3	2	6	17.17	16.18	288.8	5	1	26	7.25	7.03	189.9
4	2	6	8.87	10.06	140.0	2	2	26	20.68	23.6	89.6
3	3	6	8.82	10.30	155.2	3	2	26	4.75	3.64	274.1
1	0	10	10.08	10.01	308.2	4	2	26	6.83	6.85	275.7
2	0	10	28.35	28.20	131.9	4	3	26	6.21	6.47	192.9
3	0	10	31.79	30.83	319.5	1	0	29	30.50	27.92	227.6
4	0	10	21.42	22.00	155.1	2	0	29	3.99	5.73	99.7
5	0	10	8.60	7.60	2.8	1	1	29	10.81	9.19	111.5
1	1	10	25.88	26.06	286.5	1	0	32	15.51	16.94	52.7
2	1	10	33.49	31.76	83.6	2	0	32	41.14	41.17	242.8
3	1	10	24.18	27.05	260.5	3	0	32	35.21	34.94	76.4
4	1	10	14.22	13.73	90.5	4	0	32	11.30	11.76	275.6
2	2	10	25.87	29.20	13.5	6	0	32	9.17	6.36	110.3
3	2	10	17.47	17.68	190.3	1	1	32	36.25	36.36	245.9
1	0	13	8.62	6.98	89.4	2	1	32	41.72	40.77	99.7
2	0	13	23.44	22.57	306.0	3	1	32	17.62	20.35	304.1
3	0	13	6.63	5.54	159.1	5	1	32	6.02	7.02	161.7
1	1	13	27.09	26.56	26.1	2	2	32	27.29	24.00	332.3
2	1	13	11.42	11.49	220.0	4	2	32	7.36	6.49	210.0
1	0	16	124.38	121.23	120.5	4	3	32	6.27	6.20	97.3
2	0	16	83.14	84.51	314.4	4	0	36	8.80	5.68	2.9
3	0	16	17.98	18.10	154.7	5	0	36	6.02	8.26	195.6
4	0	16	13.50	13.68	157.1	6	0	36	8.25	6.78	35.8
5	0	16	12.08	12.20	358.1	3	1	36	5.30	5.73	152.9

Continued on the next page.

Continued.

h	*k*	*l*	|*Fo*|	|*Fc*|	*Phase*/°
4	1	36	8.96	7.40	317.6
5	1	36	7.17	7.21	135.4
3	2	36	7.22	8.41	87.5
4	2	36	7.06	7.44	259.9
4	3	36	5.51	5.18	195.3
1	0	39	55.46	5.52	88.3
2	0	39	47.59	5.60	284.6
3	0	39	11.46	0.67	75.3
4	0	39	11.45	2.49	74.1
5	0	39	9.84	1.86	255
1	1	39	55.04	1.47	358.3
2	1	39	24.14	3.13	336.5
3	1	39	5.19	5.99	165.9
4	1	39	12.52	4.19	348.1
5	1	39	5.53	0.39	93.7
3	2	39	10.8	5.97	69.1
4	2	39	6.64	1.17	269.4
1	0	45	11.08	9.98	115.9
2	0	45	7.05	5.80	311.4
1	1	45	7.85	9.92	354.2
2	0	48	11.28	11.18	170.6
3	0	48	19.91	19.28	3.8
4	0	48	16.95	16.21	196.4
1	1	48	7.54	6.85	153.3
2	1	48	16.97	16.58	13.5
3	1	48	18.32	18.16	219.4
4	1	48	10.62	10.68	61.1
2	2	48	16.03	18.35	233.7
3	2	48	12.48	12.3	84.4
1	0	52	3.90	4.04	178.6
3	0	52	9.13	8.64	281.0
4	0	52	11.57	11.51	112.0
5	0	52	9.10	8.92	308.7
2	1	52	6.81	6.19	59.2
3	1	52	10.16	10.17	230.4
4	1	52	11.59	10.25	51.8
5	1	52	6.11	5.57	247.5
2	2	52	7.35	9.30	4.3
3	2	52	11.02	9.91	169.6
4	2	52	6.30	6.61	347.9
1	0	58	51.16	49.04	259.4
2	0	58	6.21	5.86	99.9
3	0	58	17.01	16.51	104.9
4	0	58	12.18	10.53	303.9
1	1	58	16.60	16.75	155.6
2	1	58	13.28	13.27	171.4
3	1	58	12.8	15.66	6.3
2	2	58	16.65	17.01	68.2
3	2	58	7.79	6.82	262.8
3	0	64	5.26	5.42	290.8
4	0	64	10.82	8.85	124.3
5	0	64	7.59	7.81	317.6
2	1	64	4.83	5.11	273.5
3	1	64	8.64	8.02	134.9
4	1	64	9.30	8.54	342.0
5	1	64	5.15	5.62	184.6
2	2	64	7.74	7.44	136.7
3	2	64	8.60	7.82	355.8
4	2	64	5.85	5.69	208.4
2	0	68	6.66	5.90	200.7
3	0	68	12.73	11.74	28.5
4	0	68	10.04	10.1	223.2
1	1	68	5.79	6.22	350.8
2	1	68	11.52	11.82	155.2
3	1	68	11.31	12.28	332.1
4	1	68	6.45	6.67	161.5
2	2	68	12.02	13.19	83.2
3	2	68	9.54	8.75	259.4
2	0	74	23.92	22.28	20.2
3	0	74	6.24	6.95	216.2
4	0	74	5.14	5.58	221.1
1	1	74	26.48	24.12	54.0
2	1	74	13.80	12.83	257.5
4	1	74	6.89	7.19	116.4
3	2	74	7.00	7.05	170.4
2	0	84	11.50	12.59	301.9
3	0	84	12.54	12.49	137.1
4	0	84	4.09	4.60	337.8
1	1	84	8.95	9.82	69.6
2	1	84	13.04	12.70	237.5
3	1	84	6.83	7.45	58.8
2	2	84	7.41	7.87	159.0
2	0	90	9.17	9.62	306.9
3	0	90	10.86	9.93	140.5
2	1	90	12.65	11.05	165.4
3	1	90	5.82	7.03	8.2
2	2	90	7.00	7.81	40.1
2	1	100	5.79	6.73	327.5
3	0	106	4.32	4.83	69.0
2	1	106	2.93	3.46	84.7
3	1	106	4.71	4.59	288.7
2	2	106	5.61	4.04	298.8

Table IX. Atomic Fractional Coordinates and Thermal Parameters of POM Analyzed by WAXD and WAND Data Measured at Room Temperature (POM-d_2)

Atom	x/a	y/b	z/c	U_{iso}/Å^2	Atom	x/a	y/b	z/c	U_{iso}/Å^2
O01	1.0726	0.7062	−0.0012	0.057(9)	H01	1.166(11)	0.328(11)	0.0115(19)	0.081(13)
C02	1.1263	0.5208	0.0165	0.075(10)	H02	1.359(9)	0.704(10)	0.0265(17)	0.060(11)
O03	0.8752	0.3585	0.0328	0.056(10)	H03	0.649(10)	0.508(11)	0.0614(19)	0.080(13)
C04	0.8810	0.5868	0.0503	0.055(8)	H04	0.964(10)	0.851(11)	0.0418(19)	0.077(12)
O05	1.1424	0.6069	0.0689	0.053(10)	H05	1.204(14)	0.383(14)	0.0900(20)	0.096(16)
C06	1.0053	0.4035	0.0839	0.064(9)	H06	0.839(12)	0.146(13)	0.0730(20)	0.084(14)
O07	0.8035	0.4248	0.1025	0.058(10)	H07	0.776(11)	0.711(11)	0.1289(18)	0.070(12)
C08	0.9595	0.6870	0.1195	0.084(11)	H08	1.164(14)	0.899(14)	0.1180(20)	0.099(16)
O09	1.1343	0.5226	0.1370	0.070(11)	H09	1.066(11)	0.237(12)	0.1607(19)	0.073(12)
C10	0.9450	0.3542	0.1541	0.061(10)	H10	0.684(11)	0.174(11)	0.1455(19)	0.073(13)
O11	0.8705	0.5866	0.1716	0.059(10)	H11	1.365(8)	0.748(9)	0.1762(16)	0.051(10)
C12	1.1243	0.6944	0.1880	0.071(10)	H12	1.125(10)	0.904(10)	0.1936(17)	0.066(12)
O13	1.0873	0.4818	0.2060	0.063(11)	H13	0.916(13)	0.167(13)	0.2340(20)	0.087(14)
C14	0.8713	0.3828	0.2224	0.063(9)	H14	0.639(15)	0.266(14)	0.2160(20)	0.095(15)
O15	0.8998	0.6329	0.2403	0.051(9)	H15	1.350(10)	0.609(10)	0.2483(17)	0.068(12)
C16	1.1538	0.6570	0.2576	0.056(9)	H16	1.253(10)	0.907(10)	0.2666(18)	0.066(11)
O17	1.0209	0.4058	0.2747	0.047(8)	H17	0.686(13)	0.582(15)	0.2830(20)	0.090(15)
C18	0.7890	0.4779	0.2913	0.063(9)	H18	0.635(13)	0.230(13)	0.2990(20)	0.087(15)
O19	1.0012	0.7141	0.3090	0.085(13)	H19	1.159(12)	0.321(13)	0.3130(20)	0.076(14)
C20	1.1300	0.5254	0.3265	0.077(12)	H20	1.374(13)	0.737(15)	0.3320(20)	0.076(15)
O21	0.8382	0.3632	0.3439	0.052(10)	H21	0.877(14)	0.807(14)	0.3540(20)	0.085(15)
C22	0.8237	0.5756	0.3612	0.063(10)	H22	0.591(15)	0.422(17)	0.3690(20)	0.099(18)
O23	1.0652	0.6619	0.3777	0.040(8)	H23	0.907(12)	0.149(12)	0.3870(20)	0.074(14)
C24	1.0153	0.3918	0.3951	0.048(9)	H24	1.281(11)	0.466(12)	0.4070(18)	0.062(12)
O25	0.8284	0.3682	0.4127	0.059(10)	H25	0.694(13)	0.580(14)	0.4400(20)	0.084(15)
C26	0.9401	0.6157	0.4281	0.066(10)	H26	1.109(19)	0.877(19)	0.4210(30)	0.110(20)
O27	1.1467	0.6028	0.4473	0.063(11)	H27	0.812(15)	0.144(14)	0.4590(20)	0.084(16)
C28	0.9772	0.3731	0.4646	0.071(12)	H28	1.180(11)	0.321(12)	0.4754(19)	0.064(13)
O29	0.8249	0.4564	0.4808	0.039(8)	H29	1.317(13)	0.841(14)	0.4910(20)	0.082(15)
C30	1.0603	0.6936	0.4988	0.052(8)	H30	0.960(12)	0.852(11)	0.5090(20)	0.074(14)
O31	1.0838	0.4670	0.5166	0.064(12)	H31	0.577(12)	0.339(13)	0.5230(20)	0.076(14)
C32	0.8024	0.3520	0.5327	0.068(11)	H32	0.757(13)	0.124(13)	0.5388(19)	0.077(14)
O33	0.9185	0.6291	0.5509	0.047(10)	H33	1.129(14)	0.907(13)	0.5790(20)	0.084(15)
C34	1.1138	0.7034	0.5670	0.078(12)	H34	1.360(13)	0.778(15)	0.5650(20)	0.083(16)
O35	0.9588	0.3580	0.5854	0.053(10)	H35	0.636(13)	0.187(13)	0.6150(20)	0.072(15)
C36	0.8128	0.4300	0.6023	0.048(8)	H36	0.670(15)	0.546(17)	0.5940(30)	0.089(17)
O37	1.0380	0.6569	0.6205	0.064(11)	H37	1.283(11)	0.879(12)	0.6455(19)	0.071(13)
C38	1.1509	0.6173	0.6351	0.056(10)	H38	1.347(10)	0.554(11)	0.6299(17)	0.060(11)
O39	0.9393	0.3518	0.6539	0.043(9)	H39	0.603(15)	0.272(16)	0.6790(20)	0.086(16)
C40	0.8558	0.4901	0.6708	0.061(9)	H40	0.757(19)	0.670(20)	0.6630(30)	0.108(19)
O41	1.1349	0.6966	0.6887	0.058(11)	H41	1.349(10)	0.574(12)	0.7094(17)	0.060(11)
C42	1.1053	0.4801	0.7058	0.061(10)	H42	1.032(10)	0.224(11)	0.6957(18)	0.057(11)
O43	0.8028	0.4378	0.7244	0.044(10)	H43	1.153(12)	0.924(12)	0.7270(20)	0.067(13)
C44	0.9727	0.6992	0.7396	0.063(10)	H44	0.803(15)	0.764(15)	0.7440(20)	0.086(16)
O45	1.1476	0.6751	0.7577	0.041(9)	H45	0.696(14)	0.141(15)	0.7660(20)	0.085(16)
C46	0.9522	0.3685	0.7751	0.064(12)	H46	1.099(18)	0.251(18)	0.7760(30)	0.100(20)
O47	0.7998	0.5106	0.7921	0.054(10)	H47	1.269(13)	0.898(12)	0.7970(20)	0.069(15)
C48	1.0091	0.6934	0.8098	0.056(10)	H48	0.874(14)	0.819(14)	0.8130(20)	0.076(15)
O49	1.1346	0.5750	0.8262	0.055(10)	H49	0.586(13)	0.198(13)	0.8364(19)	0.068(13)
C50	0.8594	0.3505	0.8430	0.048(8)	H50	0.947(12)	0.175(12)	0.8549(18)	0.064(12)
O51	0.8143	0.5244	0.8611	0.053(10)	H51	1.370(14)	0.662(15)	0.8700(20)	0.079(17)
C52	1.1603	0.6756	0.8789	0.081(13)	H52	1.264(18)	0.932(17)	0.8820(30)	0.097(19)
O53	1.0535	0.4266	0.8956	0.060(11)	H53	0.742(12)	0.121(11)	0.9198(18)	0.056(13)
C54	0.8011	0.3740	0.9130	0.074(12)	H54	0.604(11)	0.408(13)	0.9014(19)	0.059(13)
O55	0.9824	0.6861	0.9305	0.063(11)	H55	1.240(8)	0.387(9)	0.9379(15)	0.041(9)
C56	1.1444	0.5419	0.9470	0.056(10)	H56	1.355(11)	0.764(13)	0.9575(19)	0.067(13)
O57	0.8810	0.3604	0.9653	0.043(10)	H57	0.805(14)	0.751(15)	0.9730(20)	0.082(16)
C58	0.8325	0.5525	0.9822	0.065(12)	H58	0.595(15)	0.394(18)	0.9850(20)	0.091(18)

with the observed data shown in Figure 7. Since the total number of observed X-ray reflections is too small to refine the (29/16) helix structure more accurately than that proposed in the present study. We are now trying to measure the X-ray and neutron diffraction data again to increase the total number of observed reflections furthermore.

CONCLUSION

In the present paper we measured the WAXD data at −150 °C and room temperature by using a synchrotron radiation and the WAND data at room temperature by using a highly sensitive imaging plate detector. These experiments were performed successfully for the first time in the long history of POM science.[3] The total number of X-ray reflections were increased remarkably than before by using a synchrotron facility, by which the reasonable crystal structure could be obtained including the hydrogen atomic positions. The WAND data successfully collected for the deuterated and the normal hydrogenated samples gave the hydrogen atomic positions clearly.

The structure refinement was made at first for the nonuniform (9/5) helical model to give quite reasonable and more accurate structure information than before, including the accurate hydrogen atomic positions. But, we cannot ignore the presence of another model of (29/16) helix. Though we need to investigate in more detail, it is more reasonable to consider that the POM chain takes the (29/16) helical conformation from the various experimental evidences. In fact the direct method applied to the X-ray diffraction data at −150 °C gave the reasonable model straightforwardly with acceptable reliability factor. After the structural refinement, the reliability factor was almost comparable to that analyzed for the (9/5) helical model. The WAND data measured for POM-d2 sample gave better agreement of reflection intensities to the nonuniform (29/16) model, but the total number of WAND reflections was not enough for us to decide uniquely the reasonableness of nonuniform (29/16) helix model as the final answer. In this way it is actually impossible to distinguish the superiority of these two models only through the comparison of structure factors between the observed and calculated values as long as we focus the full-rotation X-ray and neutron diffraction data. Some other experimental data, however, help us to choose the (29/16) helix as the most plausible model. As already pointed out by Carazzolo[17] and Saruyama *et al.*,[18,19] and as shown in Figure 7, the problem of uneven interlayer spacings can be solved by adopting the long repeating period of 55.710 Å, which has been confirmed for the first time by our successful observation of 001 and 002 reflections in the actual X-ray diffraction pattern (Figure 7), and a series of *00l* reflections forbidden for the (9/5) helix were reproduced reasonably on the basis of (29/16) helical model proposed by the X-ray analysis. Although the higher possibility of (29/16) helical as the best model had been proposed in the literatures,[17–19,24] we have been able to present the more quantitative and detailed result of the structural analysis for the first time on the basis of the overwhelmingly many number of observed reflections. In conclusion, the nonuniform (29/16) helical model is the best candidate which satisfies all the experimental data presented in this paper in a reasonable way. We are still investigating this problem of (29/16) helical model in more detail from such different points of view as energy calculation etc.

As described in the present paper the utilization of the synchrotron-sourced X-ray beam with very short wavelength is quite useful for observing many reflections necessary for the structure refinement of polymers. The utilization of WAND data is also very important for getting the hydrogen atomic positions with high accuracy. These information is useful for the theoretical estimation of mechanical properties on the basis of atomic coordinates and the interatomic interactions. We have already measured the X-ray and neutron fiber diagrams for the highly-oriented and fully-deuterated polymer samples such as isotactic polypropylene, polyethylene oxide, etc. The detailed structure analysis results will be reported elsewhere in a near future.

Acknowledgment. This work was financially supported by MEXT "Collaboration with Local Communities" Project (2005–2009).

REFERENCES

1. K. Tashiro, *Prog. Polym. Sci.*, **18**, 377 (1993).
2. K. Tashiro and M. Kobayashi, *Polymer*, **37**, 1775 (1996).
3. K. Tashiro, *Rep. Prog. Polym. Phys. Jpn.*, **43**, 219 (2000).
4. K. Tashiro, H. Asanaga, K. Ishino, R. Tazaki, and M. Kobayashi, *J. Polym. Sci., Part B: Polym. Phys.*, **35**, 1677 (1997).
5. K. Tashiro, K. Ishino, and T. Ohta, *Polymer*, **40**, 3469 (1999).
6. N. Sakabe, K. Nakagawa, K. Sasaki, and N. Watanabe, *Rev. Sci. Instrum.*, **60**, 2440 (1989).
7. Y. Amemiya, K. Wakbayashi, H. Tanaka, U. Ueno, and J. Miyahara, *Science*, **237**, 164 (1987).
8. C. C. Wilson, in "Single Crystal Neutron Diffraction From Molecular Materials," World Scientific Publishing Company, London, 2000.
9. N. Niimura, Y. Karasawa, I. Tanaka, J. Miyahara, K. Akahashi, H. Saito, S. Koizumi, and M. Hidaka, *Nucl. Instrum. Methods*, **A349**, 521 (1994).

10. I. Tanaka, K. Kurihara, T. Chatake, and N. Niimura, *J. Appl. Crystallogr.*, **35**, 34 (2002).
11. K. Tashiro, I. Tanaka, T. Oohara, N. Niimura, S. Fujiwara, and T. Kamae, *Macromolecules*, **37**, 4109 (2004).
12. S. Okamura, K. Hayashi, and Y. Nakamura, *Isotopes and Radiation*, **3**, 416 (1960).
13. K. Hayashi, M. Nishii, and S. Okamura, *J. Polym. Sci.*, **C4**, 839 (1963).
14. H. Tadokoro, T. Yasumoto, S. Murahashi, and I. Nitta, *J. Polym. Sci.*, **44**, 266 (1960).
15. T. Uchida and H. Tadokoro, *J. Polym. Sci., A-2*, **5**, 64 (1967).
16. Y. Takahashi and H. Tadokoro, *J. Polym. Sci., Polym. Phys. Ed.*, **16**, 219 (1978).
17. G. A. Carazzolo, *J. Polym. Sci.*, ***A-1***, 1573 (1963).
18. Y. Saruyama, H. Miyaji, and K. Asai, *J. Polym. Sci., Polym. Phys. Ed.*, **17**, 1163 (1979).
19. Y. Saruyama and H. Miyaji, *J. Polym. Sci., Polym. Phys. Ed.*, **23**, 1637 (1985).
20. G. Carazzolo, S. Leghissa, and M. Mammi, *Makromol. Chem.*, **60**, 171 (1963).
21. Y. Chatani, T. Uchida, H. Tadokoro, K. Hayahsi, M. Nishii, and S. Okamura, *J. Macromol. Sci., Phys.*, **B2**, 567 (1967).
22. L. J. Farrugia, *J. Appl. Crystallogr.*, **32**, 837 (1979).
23. G. M. Sheldrick, "Program for the Solution and Refinement of Crystal Structure," SHELX-97, University of Gottingen, Gottingen, Germany, 1997.
24. V. Gramlich, in X-ray 76, Diffraction Meeting Oxford Proceedings, PII64, S31, 1976.
25. A. Chiba, A. Hasegawa, K. Hikichi, and J. Fruichi, *J. Phys. Soc. Jpn.*, **21**, 1777 (1966).
26. V. J. McBrierty and I. R. McDonald, *J. Phys. D: Appl. Phys.*, **6**, 131 (1973).
27. Y. Takahashi and H. Tadokoro, *J. Polym. Sci., Polym. Phys. Ed.*, **17**, 123 (1979).